

Artificial Life Manuscript Submission

The Myxomatrix: Evolving Population-level Complexity in Darwinian
Artificial Life

Bradley Luke Smith ¹, Andrew Barnes ²

Corresponding: Bradley Luke Smith (brad.luke.smith@outlook.com)

1. Independent Researcher, Derbyshire, United Kingdom
2. Department of Computer Science, University of Bath, Bath, United Kingdom

Abstract. Previous attempts to replicate Darwinian evolution through artificial life simulations (ALife worlds) have struggled to achieve open-endedness or evolve population-level complexity. We suggest this limitation stems from allowing agents to survive and reproduce independently, inadvertently precluding the evolution of sophisticated collective behaviours. We propose the Interdependence Condition (IC): that agents must depend upon emergents arising at the population-level to satisfy their replication criteria reliably—a condition for encouraging population-level dynamical complexity. We introduce the Myxomatrix, an ALife world inspired by plasmodial slime moulds, and test the hypothesis that individualistic agents struggle to develop collective complexity by comparing IC-compliant and non-compliant variants. In the IC-compliant variant, agents evolve collective behaviours, progressing from Blobs to Crawlers to Sweepers, and ultimately to Switchers—populations exhibiting perception-decision-action loops that exist only at the group level and are inaccessible to the individuals, which we term superagency. These superagents develop adaptive search strategies and altruistic inter-lineage mass transfer. Conversely, in the non-compliant variant, agents typically maintain individualistic strategies (Movers) even when collective behaviours are mechanically possible, accessible through minor mutation, and demonstrably advantageous. These results suggest that the IC provides a framework for designing ALife worlds that better approximate the complexifying creative power of Darwinian evolution.

Keywords: Neuroevolution, Open-ended Evolution, Complexity, ALife Worlds, Collective Behaviour, Superagency

1 Introduction

2 Evolution by natural selection, or Darwinian evolution, explains life's prodigious diversity
3 and complexity in terms of differential survivability of genetic information, encoded
4 within imperfect replicators, over generational time. Originating with Darwin, 1859, and
5 Wallace, 1858, well before the discovery of genetic inheritance mechanisms, this concept
6 has developed into a comprehensive field with incontrovertible explanatory power as
7 successive discoveries in biology have illuminated its underlying mechanisms (Huxley,
8 1942; Rose and Oakley, 2007).

9 Beginning with relatively simple prebiotic chemistry, Darwinian evolution has progressively
10 innovated and integrated prior innovations as components of new ones at larger scales.
11 This process has gradually given rise to the highly stratified complexity we observe
12 in the biosphere today, from organic chemistry to organelles, cells, bodies, and social
13 groups (Detrain and Deneubourg, 2006). These successive organisational levels facilitate
14 emergent capabilities: metabolic regulation in organelles, motility in cells, sensorimotor
15 integration in multicellular organisms, and distributed cognitive processes in social groups
16 such as eusocial insect colonies (see Section 2). Throughout Earth's history, evolution
17 has continually generated novel forms whilst increasing the overall complexity of the
18 biosphere—a phenomenon known as open-endedness (Bedau et al., 2000; Taylor et al.,
19 2016).

20 Evolution has been harnessed by humans through the selective breeding of organisms
21 (Lush, 1943) and genetic algorithms in computer science (Goldberg, 1989; Mitchell,
22 1998), to produce animals, plants, and programs to serve targeted purposes. These
23 are supervised methods, however, where a person or human-made algorithm guides the
24 process based on some predefined output criteria and evaluation metrics. Conversely,
25 Darwinian evolution appears to possess an unsupervised creative power, where novel
26 information arises autonomously without external input, predefinition of criteria and

27 metrics, or centralised coordination. Artificial life (ALife) researchers aim to replicate
28 this phenomenon through Darwinian ALife worlds, simulated environments populated with
29 agents that (imperfectly) replicate, and compete for the prerequisite resources to do so. As
30 in nature, selection pressures arise in these systems endogenously and implicitly through
31 interactions among agents and environmental elements, in the absence of an explicit
32 fitness function.

33 Existing ALife worlds have provided insights into necessary but not sufficient prerequisites
34 for open-endedness, and demonstrated unbounded individual complexity growth (see
35 Section 3). However, open-endedness and the evolution of life-like complex dynamics
36 and intelligence remain open problems in the field (Bedau et al., 2000; Packard et al.,
37 2019). Existing systems typically model agents on real-world organisms capable of
38 independently interacting with the environment to satisfy their replication criteria. We
39 suggest this design overlooks the critical relationship between the organism (i.e., the
40 phenotype or reproducer) and the more fundamental replicator (i.e., genetic encoding
41 molecule, DNA/RNA). We conjecture that emergent effects—reliably reproduced through
42 interactions among populations of replicators—are essential for injecting novel information
43 and facilitating radical dynamical complexity growth in Darwinian worlds.

44 In this work, we introduce a novel framework for Darwinian ALife agents centered around
45 an interdependence condition (IC) that encourages population-level dynamical complexity
46 evolution. We investigate this condition through experiments in a new visually interpretable
47 ALife world: the Myxomatrix. Comparative analysis of IC-compliant and non-compliant
48 variants demonstrates that enforced interdependence reliably leads to evolved collective
49 capabilities inaccessible to the individuals, and altruistic relationships. In contrast,
50 IC-non-compliant variants frequently resulted in stunted runs with no such emergent
51 behaviors. Our findings suggest that the IC provides a valuable incipient framework
52 for designing ALife worlds that better approximate the complexifying creative power of

53 Darwinian evolution, with near-term applications in the development of intelligent agents
54 and rule-sets for multi-agent distributed computation.

55 **2 Emergence, Self-Organisation, and Complexity**

56 In large-scale systems with many interacting components, complexity can be understood
57 as an equilibrium of two opposing phenomena: emergence, where novel information not
58 present at the micro-level arises at the macro-level through interactions among micro-level
59 components; and self-organisation, where systems autonomously develop robust order
60 (i.e., repeated and sustained information). This was articulated by Lopez-Ruiz, Mancini,
61 and Calbert (1995) Lopez-Ruiz et al., 1995, and expressed mathematically by Fernández
62 et al., 2014 using Shannon's information (Shannon, 1948). Figure 1 shows the relationship
63 between emergence, self-organisation, and complexity as a function of binary string
64 composition.

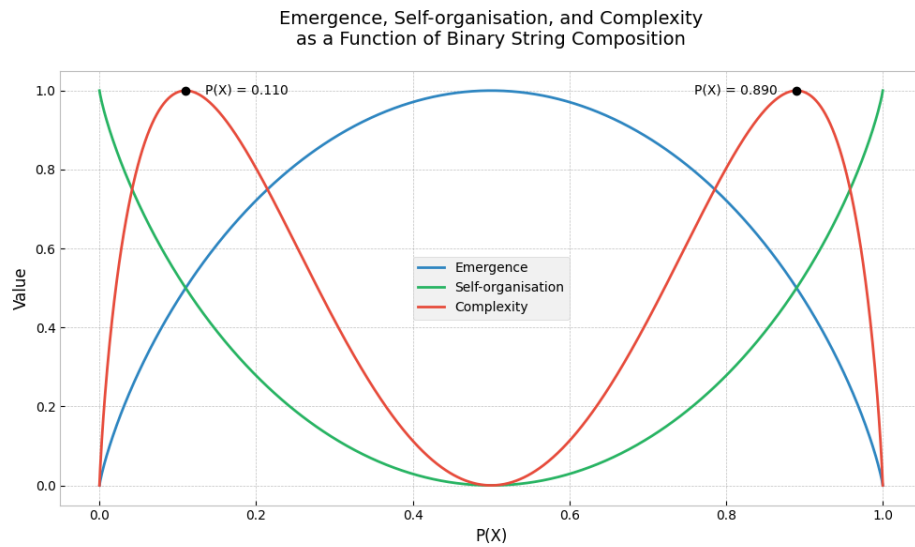


Figure 1: Emergence, self-organisation, and complexity as a function of binary string composition $P(X)$. Recreation of the analysis presented by Fernández et al., 2014, demonstrating how emergence (blue), self-organisation (green), and complexity (red) vary with binary string composition.

65 Within this framework, a maximally emergent system (where $P(X) = 0.5$) produces only
66 novel information, i.e., each state is independent of the last and therefore unpredictable.
67 Conversely, a maximally self-organising system (where $P(X) = 0$ or 1) produces entirely
68 predictable, and therefore not at all novel, information. Emergence (E) is directly inversely
69 proportional to self-organisation (S), and complexity peaks at $P(X) = 0.11$ and 0.89 , where
70 $E = S = 0.5$.

71 The natural world abounds with examples of complexity in this sense. Many small elements,
72 through their interactions distributed among the population, give rise to a gestalt entity,
73 such as cells emerging from organic molecules, representing the generation of information
74 that is novel with respect to the molecules. These entities are then reproduced to form new
75 populations at higher scales—demonstrating self-organisation through the recurrence of
76 information.

77 The interplay of emergence and self-organisation through the evolutionary process has
78 produced many strata of complexity: molecules give rise to cells, cells to bodies, and
79 bodies to superorganisms such as colonies (Detrain and Deneubourg, 2006; Gardner
80 and Grafen, 2009). This can afford novel abilities to the group that are inaccessible
81 to the micro-level elements and relevant to survival, such as the enhanced motility of
82 cells compared to organic molecules; thought, senses, and personal experience emerging
83 from nervous systems; and swarm intelligence in populations such as eusocial insect
84 colonies. Ant colonies, for instance, are capable of dynamically solving problems that
85 individual ants cannot (Bonabeau et al., 1999; Reid et al., 2011); a colony behaves as
86 an agent unto itself with perceptions, decision-making capacity, and actions, that are
87 inaccessible to the individuals. We suggest that the ability to forge stratified complexity
88 is essential for open-endedness in evolutionary systems, enabling them to outgrow their
89 initial state-space constraints by generating novel information through emergence to
90 enrich the fitness landscape.

91 3 ALife Worlds

92 ALife worlds are computer-simulated environments where programs or agents with
93 genetically encoded control mechanisms compete to survive and (near-perfectly) replicate
94 in a shared and (approximately) spatially and temporally continuous environment.
95 Selection pressures arise endogenously in the absence of an explicit fitness function,
96 attempting to reproduce life-like systems through (approximately) Darwinian evolution
97 in silico. Outstanding challenges include achieving open-endedness (i.e., perpetual
98 generation of novelty), life-like complexity amongst agents, and intelligence (Packard et al.,
99 2019).

100 Existing ALife worlds include Tierra (Ewert et al., 2013), Avida (Ofria and Wilke, 2004),
101 and Evita (Ray, 1991), which modelled programs with mutable instructions. Geb modelled
102 neural-network-controlled agents and was the first model to be classified as unbounded
103 using activity statistics (Channon, 2001), demonstrating the capacity to scale individual
104 complexity indefinitely (Channon, 2019). Chromaria (Soros and Stanley, 2014) also
105 modelled agents and demonstrated the necessity for strong coupling between the
106 phenotype and environment, such that innovations can meaningfully affect the fitness
107 landscape of other agents, for perpetuating evolutionary emergence.

108 PolyWorld (Yaeger, 1994) and the more recent Bibites (Caussan, 2020), which has brought
109 public attention to ALife, attempt to approximate nature more closely with animal- or
110 cell-like agents roaming a 2D plane, foraging for plants to sustain themselves and provide
111 fuel for replication, or hunting, fighting, and eating each other. These systems evolve
112 recognisably animal-like behaviours including following, herding, fleeing, various strategies
113 for hunting and foraging, and use of communication systems (changing body colours in
114 PolyWorld, pheromones in the Bibites). Although they produce lifelike behaviours, existing
115 ALife worlds pale in comparison to the open-ended creativity of Darwinian evolution on
116 Earth. They tend to innovate rapidly initially but eventually discover some evolutionarily

¹¹⁷ stable strategy and cease generating radically novel information.

¹¹⁸ Compared with the natural world, ALife worlds are distinctly lacking in complexity in
¹¹⁹ the sense of a confluence of emergence and self-organisation made manifest in the
¹²⁰ environment through interactions amongst populations. Only herding behaviour is
¹²¹ complex in this sense; the herd is an emergent form that dynamically reforms when
¹²² perturbed. However, as demonstrated by Hamilton, 1971, herding emerges through
¹²³ self-interest as each member attempts to hide behind the others. Complex organisms
¹²⁴ and superorganisms in nature, by contrast, are often characterised by mutualistic and
¹²⁵ altruistic relationships (West et al., 2007) between cells or individuals and, as discussed,
¹²⁶ afford agency and otherwise inaccessible abilities to populations.

¹²⁷ **4 What's Missing in ALife Worlds?**

¹²⁸ Early artificial life simulations made remarkable progress in evolving agents that exhibit
¹²⁹ animal- or cell-like behaviours, establishing foundational approaches for facilitating
¹³⁰ and measuring evolutionary emergence. Whilst metrics such as activity statistics
¹³¹ (Channon, 2001) effectively quantify individual complexity, an opportunity exists to explore
¹³² environmental complexity emerging from interactions amongst populations.

¹³³ **4.1 Reconsidering the Biological Analogy**

¹³⁴ ALife agents have traditionally been conceived as analogues to complex biological
¹³⁵ entities such as animals or cells. In nature, these are phenotypes that arise from the
¹³⁶ interaction between genetic material and environmental elements. Genetic information is
¹³⁷ encoded within replicators (DNA and the molecular machinery that accompanies it), and
¹³⁸ the phenotypes are produced—and reliably reproduced—through replicators affecting the
¹³⁹ environment according to the information they encode (the production of proteins).

¹⁴⁰ We propose that ALife agents might be better understood as 'genetic agents: expression
¹⁴¹ mechanisms, analogous to the molecular machinery that stores and translates genetic
¹⁴² information into phenotypic effects on Earth. Even in the case that ALife agents are
¹⁴³ modelled on real-world phenotypes, with abilities exceeding those of real-world replicators,
¹⁴⁴ they serve to directly express and replicate stored genetic information, rather than function
¹⁴⁵ as complex reproducing organisms.

¹⁴⁶ 4.2 Lessons from Chemical Evolution

¹⁴⁷ This re-framing suggests an interesting direction for expanding current ALife approaches.
¹⁴⁸ Early biological evolution occurred amongst molecular replicators exposed to and
¹⁴⁹ dependent upon shared chemical systems. Leading theories of life's origin, including
¹⁵⁰ replicator- and metabolism-first theories, hypothesise autocatalytic sets—networks of
¹⁵¹ molecules where each catalyses the formation of other molecules in the set, such that
¹⁵² the set as a whole can reproduce itself—as the basis for the origin of evolved complexity
¹⁵³ on Earth (Blokhuis et al., 2020; Hordijk, 2013; Jain and Krishna, 1998; Markovitch and
¹⁵⁴ Lancet, 2012; Peng et al., 2022; Plasson et al., 2011; Szathmáry and Smith, 1997).

¹⁵⁵ In these chemical systems, new innovations created by mutations in one component could
¹⁵⁶ dramatically alter the system's chemistry for all other components. Successful mutations
¹⁵⁷ did not merely benefit their host molecule but changed the evolutionary landscape for
¹⁵⁸ others dependent upon the system. This coupling between individual innovations and the
¹⁵⁹ shared environment was emphasised in Chromaria as essential for open-endedness (Soros
¹⁶⁰ and Stanley, 2014).

¹⁶¹ Theories of life's origin based in autocatalysis, considered most generally, suggest
¹⁶² the existence of two levels of complexity from the outset of evolution on Earth: the
¹⁶³ individual-level replicator, encoding genetic information that is recreated near-exactly
¹⁶⁴ in future instances; and the population-level emergent reproducer, repeatedly arising

₁₆₅ dynamics generated through interactions between replicators at scale. On Earth, the
₁₆₆ reproducer would eventually complexity into what we call the phenotype.

₁₆₇ 5 The Interdependence Condition (IC)

₁₆₈ Based on the hypothesised role of the replicator-reproducer distinction in the emergence
₁₆₉ of biological complexity on Earth, we propose the Interdependence Condition (IC) for
₁₇₀ scaffolding the evolution of population-level complexity in ALife worlds:

₁₇₁ *Agents must depend upon emergents arising through interactions amongst populations*
₁₇₂ *of agents and elements of the environment to satisfy their replication criteria reliably.*
₁₇₃ *In other words, populations of agents are networked by dependence relationships, and*
₁₇₄ *independent strategies are not viable.*

₁₇₅ Figure 2 illustrates a hypercycle, a simple hypothetical example of an autocatalytic set
₁₇₆ proposed by Eigen and Schuster, 1979, which satisfies the IC. In this system, each catalyst
₁₇₇ produces the next in a circular chain, with the final catalyst producing the first.

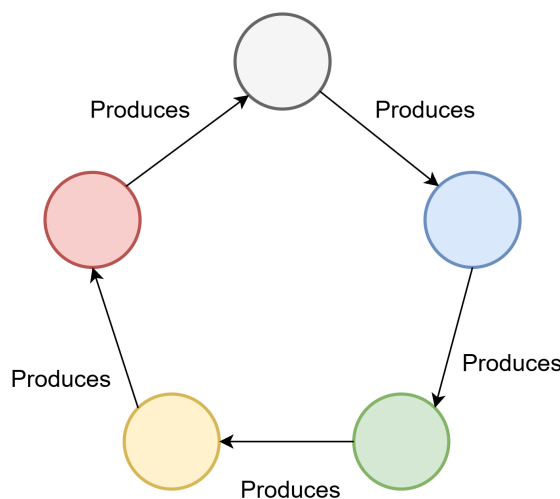


Figure 2: A diagram of a hypercycle, a simple hypothetical autocatalytic set

178 However, the IC encompasses more general forms of interdependence beyond cyclical
179 relationships. Figure 3 demonstrates an alternative configuration where the IC is satisfied
180 through linear chains of vital assistance. Here, agents provide essential support to
181 subsequent agents in the chain, culminating in a final agent that replicates multiple times
182 on behalf of the group. This architecture demonstrates how interdependence can manifest
183 without requiring multiple agent types or closed cycles.

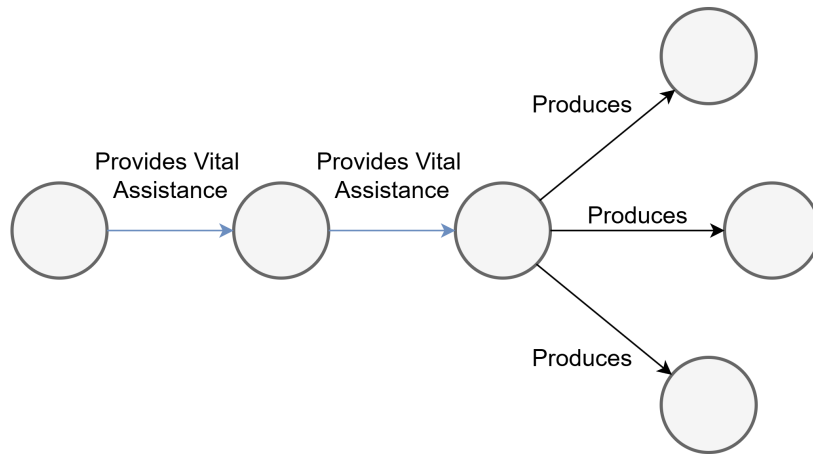


Figure 3: A chain of vital dependencies between agents, satisfying the IC

184 We hypothesise that the crucial feature of such systems is not the specific topology of
185 dependencies, but rather the reliance on population-level emergents. When populations
186 depend on emergent properties, mutations at the individual level can precipitate
187 significant changes in population-level dynamics. This mechanism provides three
188 essential features:

- 189 1. Mutable emergence generates novel information that is inherently relevant to survival
190 and replication
- 191 2. Selection pressures ensure only information advantageous to survival persists and is
192 replicated, fostering self-organisation, and therefore complexity
- 193 3. Complexity, novel but somewhat predictable information, provides novel

194 opportunities for innovation, potentially including new emergents at higher
195 scales

196 These hypothesised features suggest a mechanism for the generation and accumulation
197 of complexity: population-level emergent properties provide a substrate for evolution to
198 act upon, whilst selection ensures useful properties persist and combine in increasingly
199 sophisticated ways. However, for this process to drive increasing complexity, we propose
200 two essential implementation requirements:

- 201 1. The emergent properties that agents depend upon must arise within the shared
202 environment through local interactions between agents, directly or indirectly through
203 interaction with environmental elements
- 204 2. Mutations in individual agents must be capable of modifying the emergent properties
205 in ways that meaningfully affect the fitness landscape for agents dependent on the
206 system (i.e., affect their ability to survive, replicate, and reproduce emergents)

207 **5.1 Avoiding the Pitfalls of Independence**

208 When agents can satisfy their replication criteria independently, several problematic
209 dynamics emerge that limit the evolution of meaningful complexity. Firstly, breaks in
210 the dependency chain limit the scope of emergent effects that may arise from single
211 mutations. Individualistic agents optimise for personal survival and reproduction rather
212 than contributing to population-level dynamics that might benefit the group at potential
213 cost to themselves.

214 Secondly, agents' initial evolution optimises only for individual self-interest, rather
215 than balancing individual- with population-level pressures. Even if individualistic
216 agents develop use of communication systems, these behaviours evolve to complement
217 self-interested strategies rather than facilitate genuine collective intelligence. For agents
218 to evolve to prioritise contributing to group dynamics against self-interest, a group-based

219 strategy would need to emerge and propagate rapidly that proves more effective than
220 the previously optimised dominant individualistic strategy. In life-like simulations, this
221 transition becomes increasingly unlikely as individualistic behaviours become more
222 refined.

223 We hypothesise that individualist agents with the capacity for population-level complexity
224 struggle to develop it, as they tend to converge on evolutionarily stable (i.e., locally optimal)
225 strategies of limited complexity, tending to use communication mechanisms for ultimately
226 individualistic ends. The IC prevents this stagnation by making such individual strategies
227 non-viable from the outset, forcing evolution to explore the space of collective behaviours
228 where more sophisticated dynamics can emerge.

229 **6 A New Approach**

230 We introduce the Myxomatrix, a novel ALife world designed to test the IC and demonstrate
231 population-level complexity evolution in a visually interpretable manner. The simulation
232 draws inspiration from plasmodial slime moulds (class Myxogastria), which are large
233 multinucleate single-celled organisms that exhibit emergent swarm intelligence through
234 the coordinated actions of many nuclei distributed throughout their cytoplasm. Lacking
235 a nervous system, entirely through genetically-mediated chemical reaction cascades,
236 these organisms produce remarkably efficient networks between food sources (Boisseau
237 et al., 2016; Boussard et al., 2021). This makes them an ideal model for our
238 proof-of-concept simulation due to their simplicity and readily observable expression of
239 collective intelligence through biomass distribution.

240 The Myxomatrix operates on a 2D cellular grid where each cell may contain both a plant and
241 an agent. Agents must consume plants to acquire mass, which gradually depletes at a rate
242 proportional to their controller network complexity (i.e., the neuron and synapse counts).
243 A crucial constraint is that agents cannot move from their birth cell—only replicate into

²⁴⁴ neighbouring cells (dividing their mass equally between parent and offspring) and transfer
²⁴⁵ mass to existing neighbours. Consequently, effective environmental exploration requires
²⁴⁶ agents to develop coordinated replication and mass transfer strategies that culminate
²⁴⁷ in efficient traversal and effective search patterns at the population-level. This design
²⁴⁸ satisfies the IC through dependency chains between agents, as illustrated in Section 5,
²⁴⁹ Figure 3.

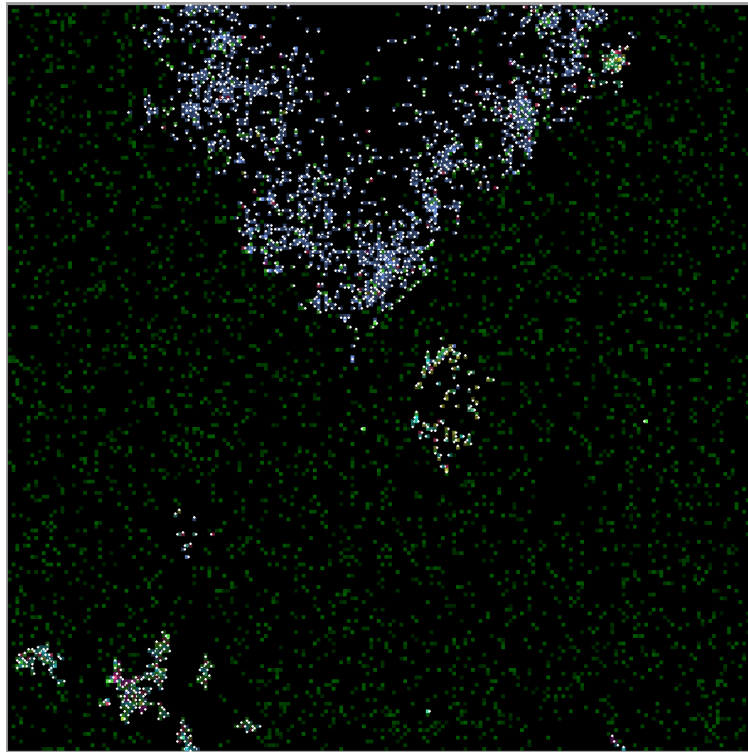


Figure 4: A snapshot of the Myxomatrix shortly after initialisation, where multiple agents have been randomly initialised into the world, showing various blob-like distribution patterns resulting from randomised replication and transfer behaviour

²⁵⁰ Figure 4 shows a snapshot of the Myxomatrix shortly after initialisation, empty cells are
²⁵¹ black, plants green, and agents various colours that approximate species (see Section 9.6).
²⁵² Agents are optionally rendered with a white dot at the centre of one of their edges, denoting
²⁵³ their orientation. These are useful when observing the Myxomatrix in video or real-time,
²⁵⁴ but can be misleading in snapshots since agents tend to rotate frequently.
²⁵⁵ Agents in the Myxomatrix implement spike-timing-dependent plasticity controller networks

256 using an encoding method based on NeuroEvolution of Augmenting Topologies
257 (NEAT) Stanley and Miikkulainen, 2002. The technical details of the Myxomatrix and the
258 controller networks are presented in Section 9 and Appendix A respectively.

259 To test the importance of the IC, we implement a control variant of the Myxomatrix
260 where agents can move between cells in addition to replicating and transferring. This
261 modification creates movement-based equivalents to all replicate-and-transfer-based
262 strategies, effectively relaxing the IC as agents can reliably satisfy their replication criteria.
263 If the IC indeed scaffolds complexity evolution, we expect to observe complex dynamics
264 emerging from replicate-and-transfer-based populations, but not from movement-based
265 ones.

266 **7 Defining Success and Experimental Design**

267 **7.1 Superagency**

268 To evaluate the Myxomatrix’s effectiveness in evolving complexity and compare
269 IC-compliant and non-compliant variants, we must establish clear criteria for non-trivially
270 complex population-level dynamics. Following the approach of Chromaria, we leverage
271 visual interpretability to identify emergent behaviours.

272 We introduce the concept of “superagency” as our primary success criterion, defined as
273 the emergence of agent groups that collectively behave as a single gestalt agent with novel
274 decision-making capabilities that:

- 275 1. Are not accessible to individual agents
- 276 2. Facilitate reproduction of group dynamics

277 Importantly, since initial agents with blank networks and randomised output biases can
278 achieve basic environmental traversal through simple replication and transfer patterns,

²⁷⁹ mere refinements of this strategy do not qualify as superagency. We seek the emergence
²⁸⁰ of novel collective capabilities beyond basic traversal, analogous to how real slime moulds
²⁸¹ can optimise network connections between food sources. Whilst our simulation draws
²⁸² inspiration from slime mould behaviour, we emphasise that exactly replicating their
²⁸³ specific behaviours is not our goal; the Myxomatrix represents a highly abstracted model
²⁸⁴ that focuses on mass-transfer-based collective intelligence.

²⁸⁵ **7.2 Experimental Hypothesis**

²⁸⁶ We hypothesise that agents in the IC-compliant Myxomatrix will reliably evolve
²⁸⁷ superagency, whilst agents in the non-compliant variant will tend to discover and
²⁸⁸ stabilise around independent strategies that preclude the emergence of complex collective
²⁸⁹ behaviours. This prediction stems from our theoretical framework suggesting that
²⁹⁰ interdependence is necessary for scaffolding the evolution of population-level dynamical
²⁹¹ complexity in artificial life systems.

²⁹² **8 Indefinite NeuroEvolution of Augmenting** ²⁹³ **Spike-Timing-Dependent Plastic Topologies** ²⁹⁴ **(INEASTDPT)**

²⁹⁵ To implement the neural controllers for agents in the Myxomatrix, we developed Indefinite
²⁹⁶ NeuroEvolution of Augmenting Spike-Timing-Dependent Plastic Topologies (INEASTDPT),
²⁹⁷ a novel variant of the NeuroEvolution of Augmenting Topologies (NEAT) algorithm (Stanley
²⁹⁸ and Miikkulainen, 2002). INEASTDPT addresses two key limitations of NEAT for artificial
²⁹⁹ life applications: the finite innovation number system that constrains long-term evolution,
³⁰⁰ and the reliance on conventional artificial neural networks rather than biologically realistic
³⁰¹ spiking neural networks.

302 INEASTDPT eliminates the global innovation counter by representing networks as paired
303 lists of neurons and synapses, with genetic compatibility determined through structural and
304 parametric comparisons rather than innovation numbers. This design enables indefinite
305 evolution. Additionally, INEASTDPT evolves spike-timing-dependent plasticity (STDP)
306 networks, providing more biologically realistic and event-driven control mechanisms
307 suited to the (approximately) spatially and temporally continuous Myxomatrix environment
308 (maass1997networks).

309 The system maintains NEAT's core evolutionary capabilities, including crossover
310 operations, structural mutations, and quantitative genetic distance measurements for
311 speciation. Agents' neural networks begin with minimal connectivity between fixed
312 input and output neurons, with hidden neurons and synaptic connections added through
313 mutation over evolutionary time. The STDP mechanisms allow synaptic weights to adapt
314 based on spike timing patterns, potentially facilitating more sophisticated learning and
315 coordination behaviours.

316 Full technical details of the INEASTDPT representation, mutation operators, crossover
317 mechanisms, and genetic compatibility calculations are provided in Appendix A.

318 **9 The Myxomatrix**

319 The Myxomatrix is a novel Darwinian ALife world designed to test the Interdependence
320 Condition (IC). Inspired by plasmodial slime molds, it models a grid-based environment
321 where agents must cooperate to explore and survive.

322 **9.1 Environment**

323 **9.1.1 Grid Structure**

324 The environment E is defined as a 2D grid of cells $C_{i,j}$, where i and j are integer
325 coordinates. Each cell can contain at most one plant and one agent.

326 **9.1.2 Time**

327 Time progresses in discrete steps $t \in \mathbb{N}$, called ticks. During each tick, all plants and then
328 all agents are updated, both in randomised order.

329 **9.2 Growth Regions**

330 Let $\mathcal{R} = R_1, \dots, R_n$ be the set of n non-overlapping rectangular growth regions, where
331 each R_i is defined by:

- 332 • **Coordinates:** $(x_{\min,i}, y_{\min,i}, x_{\max,i}, y_{\max,i}) \in \mathbb{Z}^4$, such that $x_{\min,i} < x_{\max,i}$, $y_{\min,i} < y_{\max,i}$
- 333 • **Number of plants:** $P_i \in \mathbb{N}^+$, such that $P_i < ((x_{\max,i} - x_{\min,i}) \cdot (y_{\max,i} - y_{\min,i}))$
- 334 • **Growth timer interval range:** $[\tau_{\min,i}, \tau_{\max,i}] \subset \mathbb{N}$, such that $\tau_{\min,i} \leq \tau_{\max,i}$
- 335 • **Resource regrowth range:** $[r_{\min,i}, r_{\max,i}] \subset \mathbb{R}^+$, such that $r_{\min,i} \leq r_{\max,i}$

336 **9.3 Plants**

337 Let \mathcal{P} be the set of all plants. Each $p \in \mathcal{P}$ is characterised by:

- 338 • **Position:** $(x, y) \in \mathbb{Z}^2$
- 339 • **Growth Region:** $R_p \in \mathcal{R}$, where R_p is the growth region in which plant p is located
- 340 • **Resource level:** $r_p \in [0, r_{\max,R_p}]$, where r_{\max,R_p} is the maximum resource level
341 associated with the growth region R_p

- 342 • **Growth timer:** $t_p \in [\tau_{\min, R_p}, \tau_{\max, R_p}]$, where τ_{\min, R_p} and τ_{\max, R_p} are the minimum and
 343 maximum growth timer intervals associated with the growth region R_p

344 **9.3.1 Initialisation**

345 For a new Myxomatrix simulation run:

- 346 1. $\forall R_i \in \mathcal{R}$, distribute P_i plants randomly within R_i 's boundaries.
- 347 2. $\forall p \in \mathcal{P}$, initialise $r_p \sim U(r_{\min, R_p}, r_{\max, R_p})$, where $U(a, b)$ denotes a uniform random
 348 distribution over $[a, b]$.

349 **9.3.2 Plant Dynamics**

350 At each time step:

- 351 1. **Resource Consumption:** If an agent a occupies p 's cell $C_{x,y}$ in environment E , it
 352 consumes resources from $C_{x,y}$ each tick following the rule given in Section 9.4.3.
 353 Specifically: $r_p(t+1) = r_p(t) - \min(r_p(t), c, 1 - m_a(t))$ where r_p is the resource level
 354 of the plant p , c is the consumption rate, m_a is the mass level of agent a .

- 355 2. **Movement:** If $r_p = 0$, $t_p = 0$, and no agent present:

- 356 • Move p to a random adjacent unoccupied cell within R_p
- 357 • $t_p \sim U(\tau_{\min, R_p}, \tau_{\max, R_p}) + 1$

- 358 3. **Regrowth:**

- 359 • If $t_p = 1$: $r_p \sim U(r_{\min, R_p}, r_{\max, R_p})$
- 360 • If $t_p > 0$: $t_p \leftarrow t_p - 1$

361 **9.4 Agents**

362 **9.4.1 Agent Properties**

363 Let \mathcal{A} be the set of all agents. Each agent $a \in \mathcal{A}$ is characterised by:

364 • **Position:** $(x, y) \in \mathbb{Z}^2$

365 • **Orientation:** $o \in \{\text{Northward, Eastward, Southward, Westward}\}$

366 • **Mass:** $m_a \in [0, 1] \subset \mathbb{R}$

367 • **Genetic representation:** g_a

368 • **Neural network:** N

369 • **Replication cool-down interval:** $t_r \in \mathbb{N}$

370 • **Number of communication signals:** $s \in \mathbb{N}$, denoting the number of input and output
371 neurons used for communication in each of the cardinal directions

372 **9.4.2 Neural Network**

373 The agents' controller is a spiking neural network N derived from its INEASTDPT genetic
374 representation g_a (see Appendix A):

$$N = (I, H, O, S)$$

375 where:

376 • I is the set of input neurons

377 • H is the set of hidden neurons

378 • O is the set of output neurons

379 • S is the set of synapses

380 Let $n_c \in \mathbb{N}^+$ be the parameter denoting the number of corresponding communication input
381 and output neurons, per cardinal direction, that each agent's control network possesses.

382 Input neurons I include:

- 383 • **Resource level in the current cell:** i_r
- 384 • **Presence of agents in neighboring cells:** i_a (ahead), i_l (left), i_b (behind), i_r (right)
- 385 • **Communication signals from neighbouring agents:**

386 – Ahead: $i_{ca,1}, i_{ca,2}, \dots, i_{ca,n_c}$

387 – Left: $i_{cl,1}, i_{cl,2}, \dots, i_{cl,n_c}$

388 – Behind: $i_{cb,1}, i_{cb,2}, \dots, i_{cb,n_c}$

389 – Right: $i_{cr,1}, i_{cr,2}, \dots, i_{cr,n_c}$

390 Output neurons O include:

- 391 • **Reorientation:** o_{ol} (left), o_{ob} (behind), o_{or} (right)
- 392 • **Replication:** o_{ra} (ahead), o_{rl} (left), o_{rb} (behind), o_{rr} (right)
- 393 • **Mass Transfer:** o_{ma} (ahead), o_{ml} (left), o_{mb} (behind), o_{mr} (right)
- 394 • **Communication signals:**

395 – Ahead: $o_{ca,1}, o_{ca,2}, \dots, o_{ca,n_c}$

396 – Left: $o_{cl,1}, o_{cl,2}, \dots, o_{cl,n_c}$

397 – Behind: $o_{cb,1}, o_{cb,2}, \dots, o_{cb,n_c}$

398 – Right: $o_{cr,1}, o_{cr,2}, \dots, o_{cr,n_c}$

399 **9.4.3 Agent Dynamics**

400 **1. Resource Consumption:**

$$\text{consumed} = \min(r_{x,y}(t), c, 1 - m_a(t))$$

$$m_a(t + 1) = m_a(t) + \text{consumed}$$

$$r_{x,y}(t + 1) = r_{x,y}(t) - \text{consumed}$$

401 where $r_{x,y}$ is the resource level of any plant in the agent's cell $C_{x,y}$ and $c \in \mathbb{R}^+$ is the
402 parameter denoting resource consumption rate.

403 **2. Metabolism:**

$$m_a(t + 1) = m_a(t) - M_b - M_n|H| - M_s|S|$$

404 where M_b , M_n , and M_s are parameters denoting the basal metabolic cost, the cost per
405 hidden neuron, and the cost per synapse, respectively, with $M_b, M_n, M_s \in [0, 1] \subset \mathbb{R}$.

406 **3. Reorientation:** Each agent's orientation $o \in O$ where $O = \{\text{Northward}, \text{Eastward},$
407 $\text{Southward}, \text{Westward}\}$ determines its alignment with the world axes, and by
408 extension which adjacent cells constitute the cell ahead, left, behind, and right of
409 the agent. Each of the cardinal directions represented in O is defined by relative
410 direction vectors \vec{a} (ahead), \vec{l} (left), \vec{b} (behind), \vec{r} (right), indicating the positions
411 of adjacent cells in each corresponding relative direction, relative to the agent's
412 position (x, y) , of an agent in that orientation:

- 413 • **Northward** = $(\vec{a} = (0, -1), \vec{l} = (-1, 0), \vec{b} = (0, 1), \vec{r} = (1, 0))$
- 414 • **Eastward** = $(\vec{a} = (1, 0), \vec{l} = (0, -1), \vec{b} = (-1, 0), \vec{r} = (0, 1))$
- 415 • **Southward** = $(\vec{a} = (0, 1), \vec{l} = (1, 0), \vec{b} = (0, -1), \vec{r} = (-1, 0))$
- 416 • **Westward** = $(\vec{a} = (-1, 0), \vec{l} = (0, 1), \vec{b} = (1, 0), \vec{r} = (0, -1))$

417 If one or more of the agent's reorientation output neurons O_{ol}, O_{ob}, O_{or} fire, select
 418 one of the fired neurons uniformly at random. Then:

$$o = O_{(o+\Delta) \bmod 4}$$

419 Where:

- 420 • If $O_{\vec{o_l}}$ is selected (turn left): $\Delta = 3$ (equivalent to -1)
- 421 • If $O_{\vec{o_b}}$ is selected (turn back): $\Delta = 2$
- 422 • If $O_{\vec{o_r}}$ is selected (turn right): $\Delta = 1$

423 4. **Replication:** Let the agent's metabolic rate be $m_a = M_b + M_n|H| + M_s|S|$, where $|H'|$
 424 and $|S'|$ are the number of hidden neurones and synapses in it's network, respectively.

425 The replication threshold is given by:

$$m_r = C_r + S_r \cdot (2 \cdot m_a)$$

426 where $C_r \in \mathbb{R}^+$ is the replication cost, $S_r \in \mathbb{R}^+$ is the replication survivability scalar
 427 parameter, and $m_{a'}$ is the offspring's metabolic rate as defined above. This enures
 428 that both the parent and offspring can survive for S_r ticks after replication.

429 If $m_a > m_r$, $t_r = 0$, and one or more of the agent's replication neurons $o_{ra}, o_{rl}, o_{rb}, o_{rr}$
 430 fire, select one of the fired neurons uniformly at random. For the selected neuron, let
 431 $\vec{d} = (d_x, d_y) \in o$ be the corresponding relative direction vector:

- 432 • If the cell $C_{x+d_x, y+d_y}$ in direction d contains no agent: create a new agent a' in
 433 cell $C_{x+d_x, y+d_y}$
- 434 • Orient a' :
 - 435 - If $d = (0, -1)$: set $o' = \text{Northward}$

436 - If $d = (1, 0)$: set $o' = \text{Eastward}$

437 - If $d = (0, 1)$: set $o' = \text{Southward}$

438 - If $d = (-1, 0)$: set $o' = \text{Westward}$

439 such that a' initially faces away from its parent a

440 • Set $m_a(t + 1) = m_{a'} = \frac{m_a(t) - C_r}{2}$

441 • Mutate $g_{a'} = \text{Mutate}(g_a)$ with probability p_m

442 • Set $t_r = t_c$ for both a and a'

443 where $t_c \in \mathbb{N}$ is the cool-down time parameter.

444 If $t_r > 0$: $t_r = t_r - 1$

445 5. **Mass Transfer:** For each relative direction vector $\vec{d} = (d_x, d_y) \in o$, if o_{md} fires and
446 the adjacent cell $C_{x+d_x, y+d_y}$ contains an agent b that is genetically compatible with a
447 $\text{Compatible}(g_a, g_b)$:

$$\text{transferred} = \min(m_a(t), r_t, 1 - m_b(t))$$

$$m_a(t + 1) = m_a(t) - \text{transferred}$$

$$m_b(t + 1) = m_b(t) + \text{transferred}$$

448 where r_t is the transfer rate parameter.

449 If mass is transferred between a and b , apply crossover with parameter probability
450 $p_c \in [0, 1] \subset \mathbb{R}$:

$$g_a, g_b = \text{Crossover}(g_a, g_b)$$

451 6. **Communication:** For each relative direction vector $\vec{d} = (d_x, d_y) \in o$, if any of
452 the communication output neurons $o_{cd,1}, o_{cd,2}, \dots, o_{cd,n_c}$ fire, and the adjacent cell

453 $C_{x+d_x, y+d_y}$ contains an agent b that is genetically compatible with a Compatible(g_a ,
 454 g_b): Send a spike to the corresponding input neuron $i_{cd,1}, i_{cd,2}, \dots, i_{cd,n_c}$ of agent b .

455 **9.5 IC-non-compliant Variant**

456 In the IC-non-compliant variant, agents gain movement capability but share a single action
 457 timer between movement and replication. The replicate action from Section 9.4.3 is
 458 replaced with the following movement-enabled action logic:

459 For an agent a with mass m_a , movement outputs $o_{ma}, o_{ml}, o_{mb}, o_{mr}$ and replication outputs
 460 $o_{ra}, o_{rl}, o_{rb}, o_{rr}$, when action cooldown $t_a = 0$:

461 Let $\vec{D} = \{\text{ahead, right, behind, left}\}$ be the set of possible directions relative to the agent's
 462 orientation. For each direction $\vec{d} \in \vec{D}$ at index i :

463 If target cell $C_{x+d_x, y+d_y}$ contains no wall and no agent:

464 • If $o_{m\vec{d}}$ and $m_a > c_m$, add (move, i) to valid actions

465 • If $o_{r\vec{d}}$ and $m_a > m_r$, add (replicate, i) to valid actions

466 where $c_m \in \mathbb{R}^+$ is the movement cost parameter.

467 If valid actions exist, randomly select one (action, i):

468 If action = move:

469 • Set agent orientation $o = O_{(o+i) \bmod 4}$ where O is the ordered set of orientations

470 • Update agent position to target cell: $(x, y) \leftarrow (x + d_x, y + d_y)$

471 • Set $m_a(t+1) = m_a(t) - c_m$

472 • Set $t_a = t_c + 1$

473 If action = replicate:

474 • Create new agent a' in target cell with:

475 – Orientation $o' = O_{(o+i) \bmod 4}$

476 – Mass $m_{a'} = m_a = \frac{m_a(t) - c_r}{2}$

477 – Genome $g_{a'} = \text{Mutate}(g_a)$ with probability p_m

478 • Set $t_a = t_c + 1$ for both a and a'

479 If $t_a > 0$: $t_a = t_a - 1$

480 where $t_c \in \mathbb{N}$ is the action cooldown parameter. This modification allows agents to either

481 move or replicate but maintains a shared cooldown timer between these actions.

482 9.6 Species Colouration

483 The species manager S maintains a list of progenitor genetic representations:

$$S = \{(g_1, c_1, A_1, n_1), \dots, (g_k, c_k, A_k, n_k)\}$$

484 where g_i is a progenitor representation, c_i is its associated colour, A_i is the set of living

485 agents of that species, and n_i is a count.

486 For a new agent a :

487 1. Find i such that $\text{Compatible}(g_a, g_i)$

488 2. If found: add a to A_i and increment n_i

489 3. If not found: create new entry $(g_a, \text{RandomColour}(), \{a\}, 1)$ in S

490 4. If n_i reaches parameter threshold $n_\theta \in \mathbb{N}^+$: update $g_i = g_a$

491 Remove entries where A_i becomes empty.

492 **9.7 Parameters**

Parameter	Value	Parameter	Value
Consumption Rate (c)	0.5	Transfer Rate (r_t)	0.2
Basal Metabolic Cost (M_b)	0.001	Crossover Probability (p_c)	0.2
Neuron Cost (M_n)	0.0002	Mutation Probability (p_m)	0.08
Synapse Cost (M_s)	0.00002	Compatibility Threshold (θ)	0.16
Replication Survivability (s_r)	6.0	Communication Signals (n_c)	4
Replication Cost (c_r)	0.01	Progenitor Threshold (n_θ)	500
Movement Cost (c_m)	0.01		
Action Cooldown (t_c)	6		

Table 1: Model Parameters and Their Values

493 **10 Results**

494 In this section, we provide comparative analysis of the qualitative graphical and
495 quantitative behavioural data outputs of IC-compliant and non-compliant Myxomatrix runs.
496 First, we outline visually observable trends in both variants separately, then compare the
497 behavioural data from both.

498 **10.1 The IC-compliant Myxomatrix**

499 Movement actions are disallowed in the IC-compliant Myxomatrix. To search for food,
500 agents must therefore rely on lineage-level traversal patterns emerging through cohesive
501 behaviours and predictable interactions among agents. This design satisfied the IC in the
502 dependency chain manner depicted in Section 5, Figure 3.

503 **10.1.1 Blobs**

504 When initialising the simulation, a single agent is initialised into a random position. Its
505 freshly initialised INEASTDPT genome codes for a network with no hidden nodes and
506 randomised biases on the fixed input and output nodes. This results in a stochastic firing
507 pattern on the output nodes, which most often produces erratic replication and transfer
508 actions by the agent.

509 When an erratic agent replicates into a neighbouring cell containing a plant, the daughter
510 agent will consume the plant and begin erratically replicating and transferring too. This
511 gives rise to a population-level pattern we refer to as Blobs, which expand as sections of
512 their undulating perimeters happen across plants. Agents at the centre of large Blobs will
513 consume all available plants and perish before they regrow, causing large Blobs to split into
514 smaller ones. A Blob can only expand into areas not recently searched and thus densely
515 populated with plants, so tend to perish when they reach a dead end at the world border.

516 Nonetheless, a single randomly initialised agent will often give rise to a self-sustaining
517 population of agents forming Blobs. Sometimes, the initial agent performs insufficient
518 replication and transfer actions to produce a self-sustaining population, and all agents
519 perish. These runs were discarded. The Myxomatrix's setup interface allows for multiple
520 agents to be each randomly initialised into the world, increasing the probability that one
521 will flourish and evolution can begin.

522 Blobs are very inefficient searchers. They perform redundant replication and transfer
523 actions, passing mass back and forth without traversing, and cannot cross recently
524 searched areas. These inefficiencies were consistently addressed in all 20 IC-compliant
525 runs as they progressed through 3 further phases of behavioural development, beginning
526 with Crawlers.

527 **10.1.2 Crawlers**

528 The redundant actions of Blobs, like transferring mass back and forth or traversing in
529 tight loops, are gradually eliminated. This produces what we call Crawlers: a single agent
530 replicates once and transfers all its mass to its offspring. The offspring do the same,
531 repeatedly, until the lineage runs out of mass or an agent is produced into a cell containing
532 a plant. The agent then consumes mass from the plant and replicates in multiple directions,
533 creating many new crawlers. The effect is a branching, long-range search pattern. We call
534 them Crawlers because they appear to expand and contract like a crawling worm.

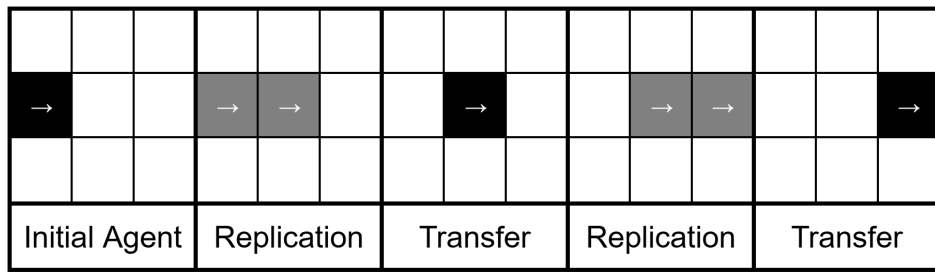


Figure 5: A depiction of a traversing Crawler

535 Figure 5 depicts a Crawler where each agent replicates and transfers ahead, creating
536 offspring facing the same direction as the parent. An equivalent pattern often forms
537 through leftward/rightward replication followed by opposite-side reorientation.

538 Crawlers quickly outcompete Blobs through faster searching and their ability to cross
539 gaps between plant clusters. By consuming plants at the Blobs' edges, they drive them
540 to extinction. Once Crawlers dominate, the population size stabilises.

541 **10.1.3 Sweepers**

542 Next emerge Sweepers. These behave like Crawlers but replicate consistently to one
543 side as well as ahead. This creates a diagonal line of Crawler-like lineages traversing
544 in formation, as shown in Figure 6.

545 Since Sweepers spread mass across multiple Crawler-like lineages, they achieve a shorter

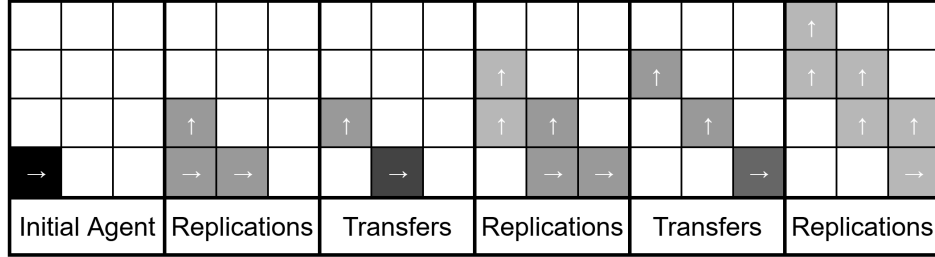


Figure 6: A depiction of a flourishing Sweeper

range but more thorough local search. We observed various Sweeper patterns: multiple short Sweepers created following a circular pattern and traversing in different directions, single long sweepers, and slow-traversing horizontal/vertical lines that act as walls and are sustained by donations of mass. Sweepers always emerge, typically within 50,000 ticks, though sometimes they form short diagonal lines of only 2-3 cells. They regularly merge and reform, and do so more effectively as evolution progresses.

Though Sweepers are a clear population-level pattern that emerges consistently, it is a trivial one, like the herding behaviour discussed in Section 3. Each lineage benefits from being near others, but Sweepers develop no mutualistic or altruistic relationships, nor gain any new abilities beyond more efficient search.

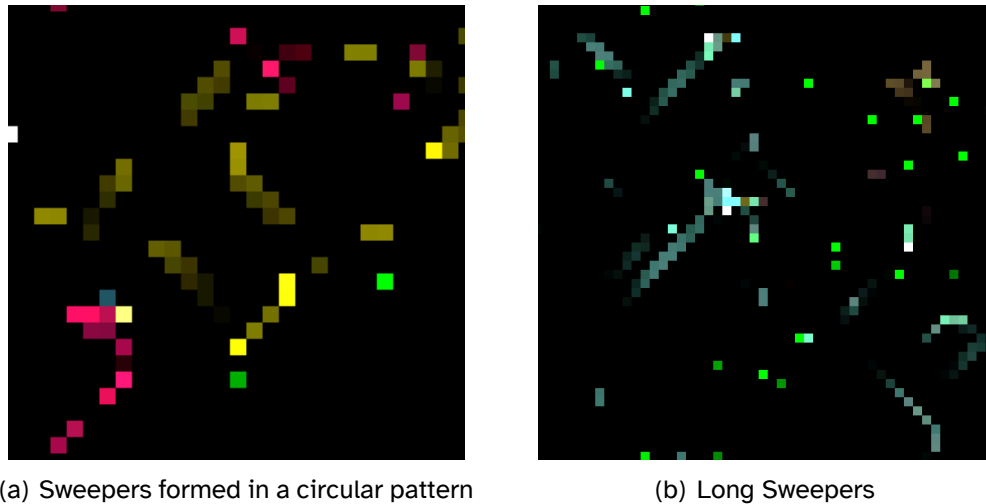


Figure 7: Snapshots of the Myxomatrix showing Sweepers

556 **10.1.4 Switchers**

557 Long Sweepers reliably evolve into Switchers—modified Sweepers that transfer mass
558 between lineages after replication. In the clearest cases, mass flows from the oldest to
559 the youngest lineage. In Figure 6’s Sweeper, each agent transfers mass right and ahead,
560 concentrating the line’s mass in the rightmost agent.

561 This innovation solves two key problems with Sweepers. First, it addresses wasted mass:
562 in Sweepers, agents that cannot afford to replicate remain in their cell until they starve,
563 briefly dropping from formation before dying. Switchers solve this by having agents die
564 when they transfer their mass to a neighbouring lineage, preserving the mass. This creates
565 the appearance of Crawlers expanding into Sweepers, then collapsing back down.

566 Second, it enables adaptive search based on collected mass. After collapsing, the final
567 lineage’s mass level determines behaviour. With low mass (indicating few nearby plants),
568 the final agent acts as a Crawler, traversing further than separate lineages could manage
569 since it operates with a single metabolism. With high mass (indicating multiple plants
570 found during the sweep), the agent creates a new Sweeper-like diagonal line traversing
571 perpendicularly to the first.

572 This adaptive mechanism allows Switchers to dynamically choose between long-range
573 Crawler-like search and short-range Sweeper-like patterns based on local resource
574 distribution. Individuals are not able to perceive this information, so this evolved
575 population-level decision making ability qualifies Switchers as superagents.

576 Switchers are most easily identified when they evolve from long Sweepers and collapse
577 down to a single lineage. They are not easily captured in snapshots, appearing usually
578 as either a Crawler or Sweeper, but can sometimes be captured as one Sweeper-like line
579 emerging from the end of another.

580 Some Switchers collapse into multiple Crawler-like lines, which can create a very busy



Figure 8: Snapshots of the Myxomatrix showing Switchers

581 environment with numerous collisions. Likewise, agents in some runs replicate and transfer
 582 infrequently, effectively waiting for plants to grow in front of them. In others, many small
 583 Sweepers are produced rather than one large one. Identifying consistent superagent
 584 behaviours visually in these busy runs is difficult as patterns are often perturbed.

585 10.2 The IC-non-compliant Myxomatrix

586 In the IC-non-compliant Myxomatrix, the randomisation of biases on initial agents' output
 587 neurons produces a greater range of emergent behaviours. Some initial agents make no
 588 use of movement actions, others move exclusively and fail to propagate due to never
 589 replicating. Most commonly, replication, transfer, and movement actions are combined,
 590 resembling the Blobs from the IC-compliant variant except that agents occasionally detach
 591 from the Blob perimeter through movement. One of two strategies tends to arise: either
 592 agents stop moving and traverse primarily through replication and transfer, evolving
 593 as in the IC-compliant variant thereafter; or they traverse primarily through movement,
 594 finding plants independently without requiring mass transfer from other agents. We term
 595 these movement-based strategies “Movers”. Runs where movement actions disappear
 596 before a population of independently viable agents is established are discounted from
 597 this investigation. We analysed 20 runs where Movers successfully established each for
 598 750,000 ticks, or until a pure replicate/transfer-based strategy emerged.

599 Unlike Crawlers' unidirectional movement, Movers typically traverse in various directions
600 and form diffuse and erratic populations rather than moving in formations. Our analysis
601 revealed that this basic Mover strategy can be evolutionarily stable, persisting unchanged
602 throughout the full 750,000 ticks in 7 of the 20 runs.

603 In 7 other runs, Movers developed hybrid strategies through two distinct patterns: some
604 combined replication/transfer with movement in their traversal pattern, while others used
605 replication and transfer to distribute mass from plant cells before separating into individual
606 Movers. Figure 9 shows a common hybrid formation we term "Diffuse Sweepers"—agents
607 that sweep across the environment in diagonal or horizontal/vertical formations whilst
608 maintaining one-cell gaps between lineages, alternating between replication/transfer- and
609 movement-based traversal.

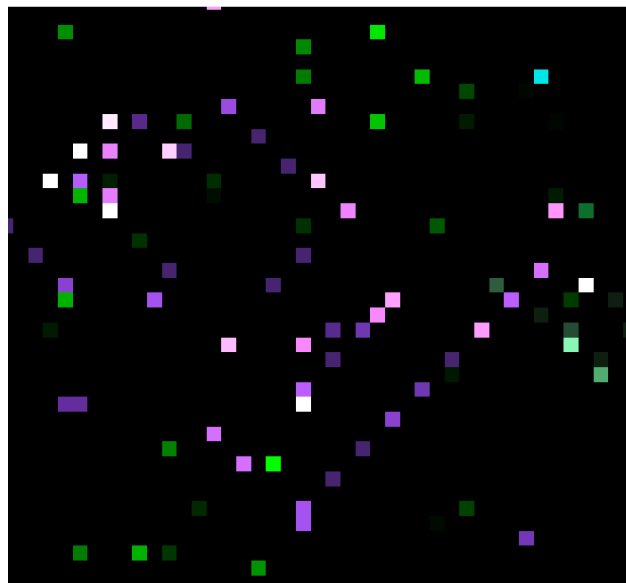


Figure 9: A snapshot of the IC-non-compliant Myxomatrix featuring Diffuse Sweepers forming intermittent diagonal lines

610 These hybrid strategies characteristically maintain separation between agents, preventing
611 inter-lineage mass transfer. In all 7 runs where hybrid strategies arose from a population
612 of movers, they did so within the first 100,000 ticks, then maintained the strategy for the
613 remainder of the 750,000 ticks without developing superagent capabilities.

614 Mutations producing Crawler- and Sweeper-like formations among established Movers
615 were observed to fail when mutated agents donated mass to closely related non-mutated
616 agents, effectively eliminating the formation-based allele while promoting the competing
617 individualistic strategy. Other populations adapted by developing hybrid strategies like
618 Diffuse Sweepers, reaching a new stable state. In some runs, however, initially stable
619 Movers gradually incorporated more replication and transfer actions until becoming
620 Crawlers, and evolving as in the IC-compliant variant thereafter. Notably, superagency
621 emerged only from replication/transfer-based strategies; we never observed groups
622 moving in close formation whilst exchanging mass.

623 10.3 Comparative Analysis of Agent Metrics

624 In this section we compare the change in the following agent metrics:

- 625 • Population size per tick
- 626 • Mean units of mass transferred per agent per tick
- 627 • Mean number of replications per agent per tick
- 628 • Mean number of movement actions taken per agent per tick
- 629 • Mean number of synapses per agent neural network per tick
- 630 • Mean number of neurons per agent neural network per tick
- 631 • Mean number of communication actions taken per agent per tick
- 632 • Mean number of reorientation actions taken per agent per tick

633 The IC-non-compliant runs are clustered as below, and metrics for each cluster are
634 displayed on independent plots:

- 635 • **Abandoned Movement:** Runs that were visually identified as having disused
636 movement actions and manually terminated within 750,000 ticks

- 637 • **Pure Mover:** 750,000 tick runs where mass transfer per agent, averaged over all
 638 ticks, is ≤ 0.005
- 639 • **Hybrid:** 750,000 tick runs where mass transfer per agent, averaged over all ticks, is
 640 > 0.005

641 **10.3.1 Mass Transfer**

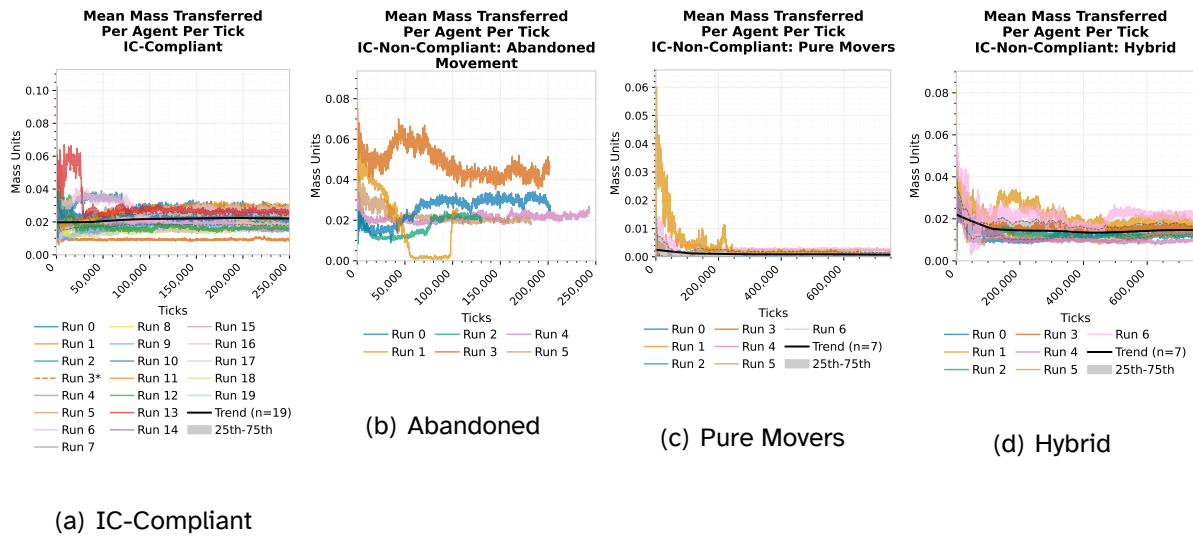


Figure 10: Average mass transferred per agent (larger graphs in Appendix B)

642 In IC-compliant runs, as shown in the leftmost plot of Figure 10, following a brief initial
 643 period of instability, the mass transfer rate stabilised at ~ 0.025 mass units transferred per
 644 agent per tick on average (note that each agent can store a maximum of 1 unit each, but
 645 often has far less, with intervals of many ticks between transfers). In IC-non-compliant
 646 worlds where movement was abandoned, the second plot shows a longer period of
 647 instability before settling into replicate-transfer-based strategies within the first 100,000
 648 ticks.

649 The pure Mover and hybrid strategies shown in the third and fourth plots, respectively,
 650 demonstrate distinctive transfer patterns. One pure Mover run (Run 1) begins with a
 651 relatively high mass transfer rate, and eliminates it gradually over the first 300,000 ticks.

652 All other pure Mover runs begin with transfer rates lower than the initial IC-compliant
 653 or abandoned movement runs (~ 0.002 : 0.02 units), which decrease rapidly and plateau
 654 at ~ 0.001 units. Hybrid runs tended to begin with a transfer rate of ~ 0.02 units, as in
 655 IC-compliant and abandoned movement runs, which gradually diminishes and plateaus at
 656 ~ 0.012 units.

657 The differences in initial agent mass transfer patterns, and that movement abandonment
 658 only occurs within the first 100,000 ticks, strongly indicates that the transfer behaviour
 659 of the initial agent is crucial for the evolvability of the 3 strategies in IC-non-compliant
 660 worlds.

661 10.3.2 Replication

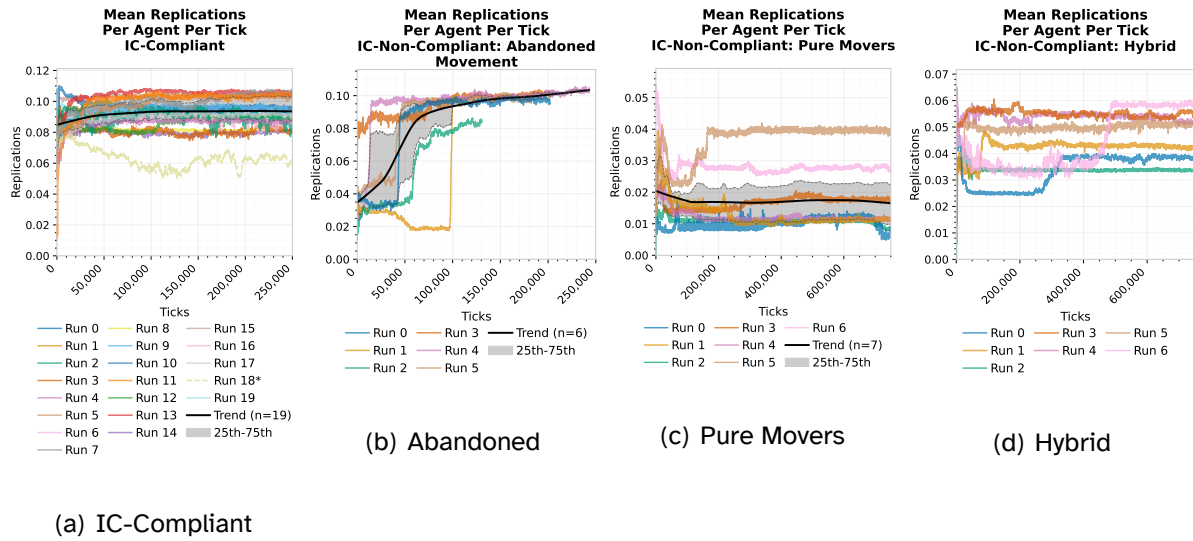


Figure 11: Average replications per agent (larger graphs in Appendix B)

662 In IC-compliant runs (leftmost plot), the replication rate consistently rose slightly for
 663 the first $\sim 40,000$ ticks, then plateaued at $\sim 9\%$ of agents replicating per tick. In
 664 IC-non-compliant worlds where movement was abandoned (second plot), sudden steep
 665 increases in the replication rate indicate rapid transitions away from the Mover strategy
 666 following the occurrence of a critical mutation within the first 100,000 ticks. The

667 transitioned agents tend to evolve and plateau similarly to IC-complaint ones thereafter.
 668 The pure Mover and hybrid strategies (third and fourth plots, respectively) express a wider
 669 range of replication rates than IC-complaint and abandoned movement runs. Hybrid
 670 strategies tend to replicate approximately half as often as agents in IC-complaint runs,
 671 and pure Movers predominantly less still.

672 10.3.3 Movement

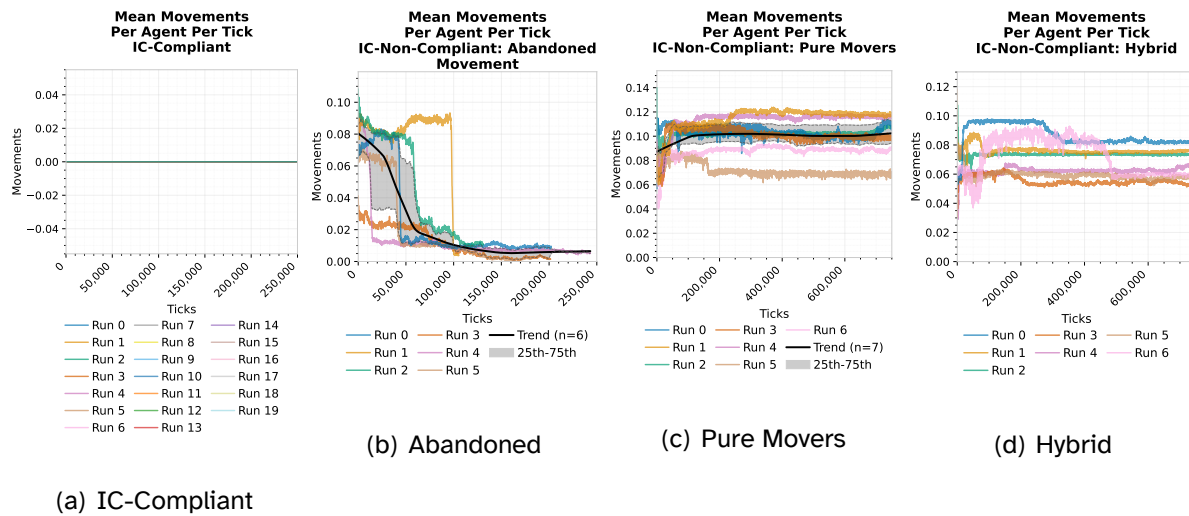


Figure 12: Average movements per agent (larger graphs in Appendix B)

673 Movement rates in the IC-non-complaint runs are approximately inversely proportional to
 674 the replication rates (see previous subsection), showing steep drops when movement is
 675 abandoned, and a wider range of strategies in pure Mover and hybrid strategies.

676 **10.3.4 Population Size**

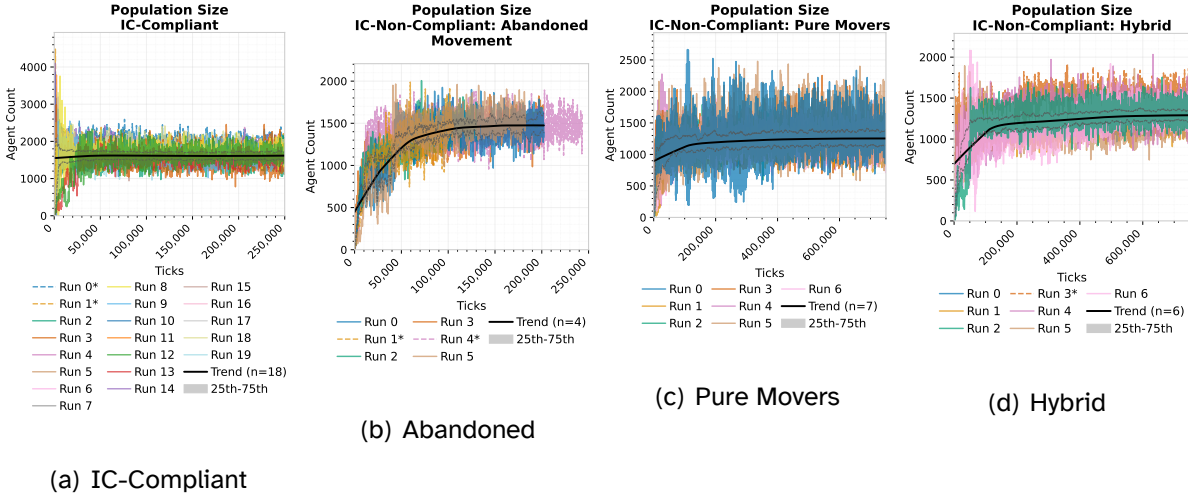


Figure 13: Population size over time (larger graphs in Appendix B)

677 In IC-complaint runs, population size initially fluctuates rapidly while the agents are in
 678 the Blob phase. This stabilises within the first $\sim 50,000$ ticks as redundant actions
 679 are removed and crawlers/sweepers arise. Compliant runs exhibit a range of initial
 680 population sizes, but these all converge at ~ 500 agents on average following the unstable
 681 Blob phase. In non-compliant runs, this initial instability is less pronounced, which
 682 is expected given their increased tendency to diffuse. Abandoned movement runs in
 683 particular show relatively slight initial fluctuations, calling for further investigation into
 684 agent characteristics in the early stages of evolution in these runs.

685 Again, we see consistent differences in the initial conditions between non-compliant
 686 clusters. Runs where movement was abandoned tended to express small early population
 687 sizes of ~ 500 agents. Pure Mover and Hybrid strategies expressed sizes of ~ 900 and
 688 ~ 700 respectively. This supports the idea that individualists can cut themselves off
 689 from easily accessible (through mutation) cooperative strategies as they optimise their
 690 individualist strategy; the less prolific Movers were more susceptible to being supplanted
 691 by cooperative mutants than those Movers initialised with more effective search strategies.

692 **10.3.5 Synapses**

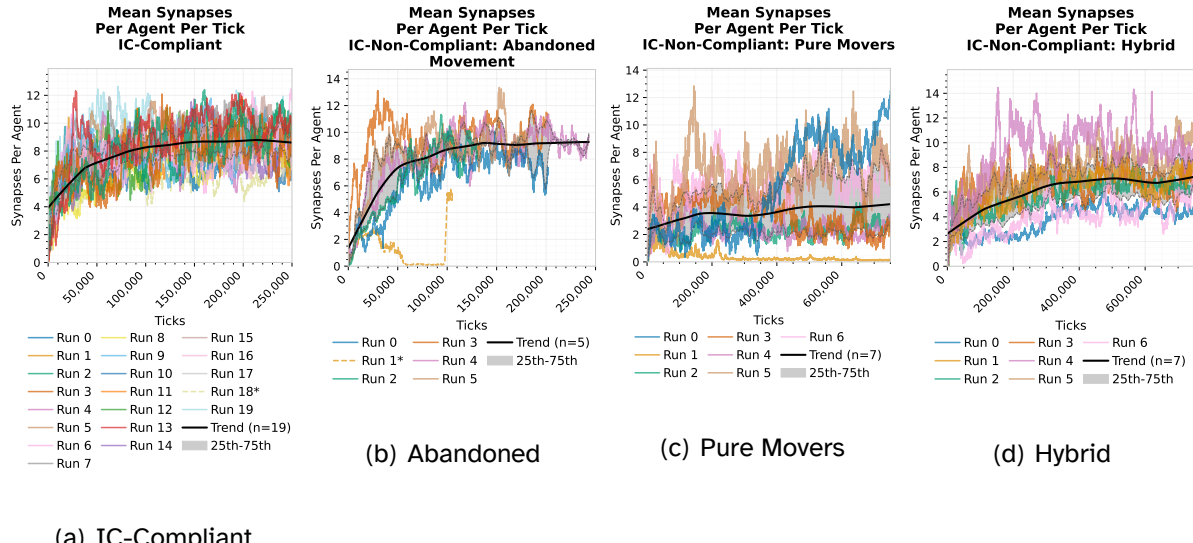
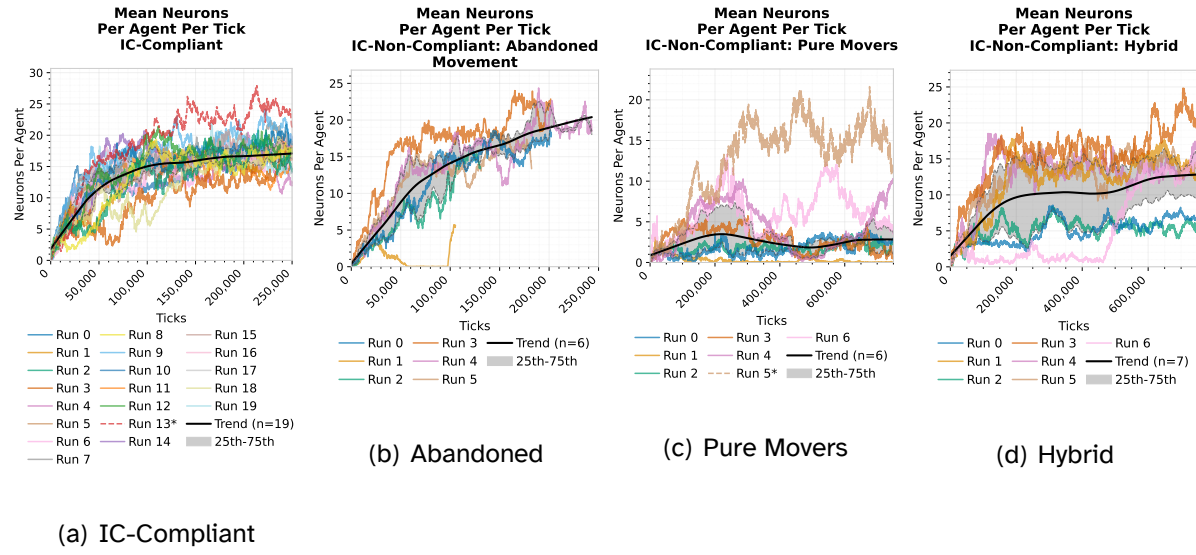


Figure 14: Average number of synapses per agent (larger graphs in Appendix B)

693 In IC-compliant runs, the average number of synapses in agent neural networks increases
 694 for 30,000 ticks, then plateaus at a mean of ~ 8 across all 20 runs (leftmost plot). Within
 695 each run, the number of synapses rises and falls sharply over tick time. Pure movers tend
 696 to plateau with the fewest synapses, averaging ~ 4 (third plot), while hybrids average ~ 6
 697 (fourth plot). Synapses cost mass to maintain, so we would expect unnecessary synapses
 698 to be eliminated over evolutionary time. That IC-compliant runs consistently evolve greater
 699 network complexity than non-compliant runs, therefore, suggests that IC-compliant agents
 700 exhibit more computationally demanding behaviours. This appears to be true of the
 701 harder-to-observe busy runs too.

702 **10.3.6 Hidden Neurons**



(a) IC-Compliant

Figure 15: Average number of neurons per agent (larger graphs in Appendix B)

703 In each cluster, the number of hidden neurons per agent follows a very similar trend to
 704 synapses (see previous section). Interestingly, agents tended to evolve, on average, more
 705 neurons than synapses, proportional to their replication rates. Only pure Movers tended
 706 to possess an equal number of neurons and synapses, with the single anomalous pure
 707 Mover run (Run 6) exhibiting increased replication rates and also greatly more neurons
 708 than synapses.

709 Possessing more neurons than synapses guarantees that some neurons will serve no
 710 function, as they have no output connections. Over generational time, we should therefore
 711 expect excess neurons to be eliminated. The persistence of excess neurons and their
 712 relationship to replication rates indicate that the INEASTDPT mutation rate parameters
 713 used regularly create new neurons only to then remove their synapses. This likely occurs
 714 because the new neurons caused adverse effects that were resolved by synapse rather
 715 than neuron deletion mutations. This observation suggests a need to adjust the mutation
 716 protocols or rate parameters for neuron and synapse creation and deletion, or perhaps to
 717 make these parameters mutable themselves.

718 **10.3.7 Communication**

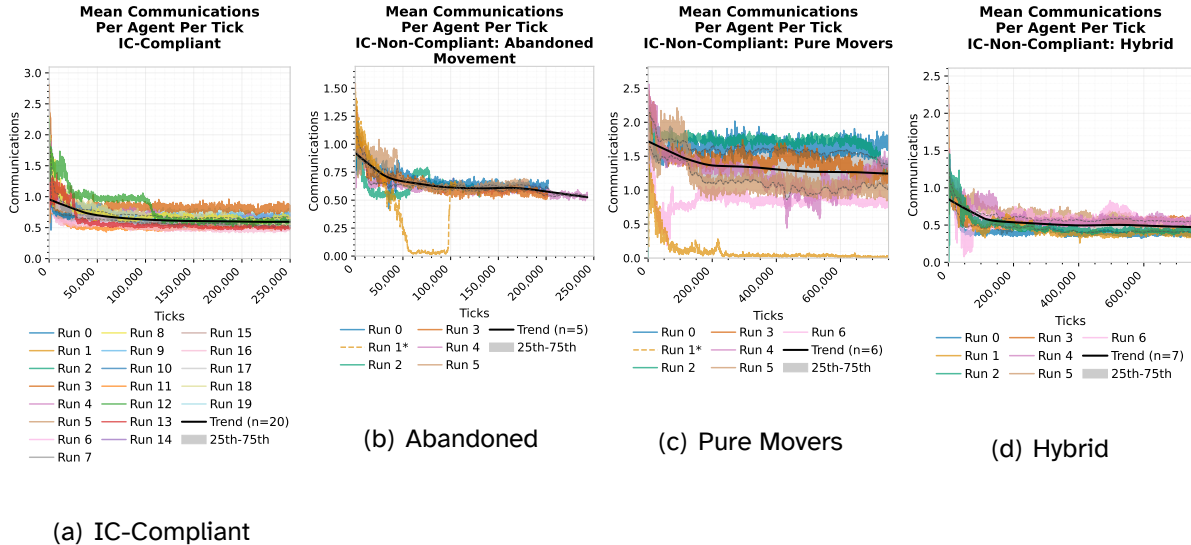


Figure 16: Average communications per agent (larger graphs in Appendix B)

719 In all runs, use of communication signals tended to decrease initially, then plateau and
 720 show reduced variability. Note that communication signals are counted whether or not
 721 another agent receives them, and producing them incurs no mass cost. IC-compliant,
 722 abandoned movement, and hybrid runs all follow very similar trends, while pure Movers
 723 showed much greater variability in plateaued communication rates. If agents did not
 724 make use of communication inputs within their networks, we would expect use of
 725 communication signals to fluctuate randomly through genetic drift. The predictability of
 726 communication trends in non-Movers suggests communication is utilised to coordinate
 727 replication-and-transfer actions.

728 **10.3.8 Reorientation**

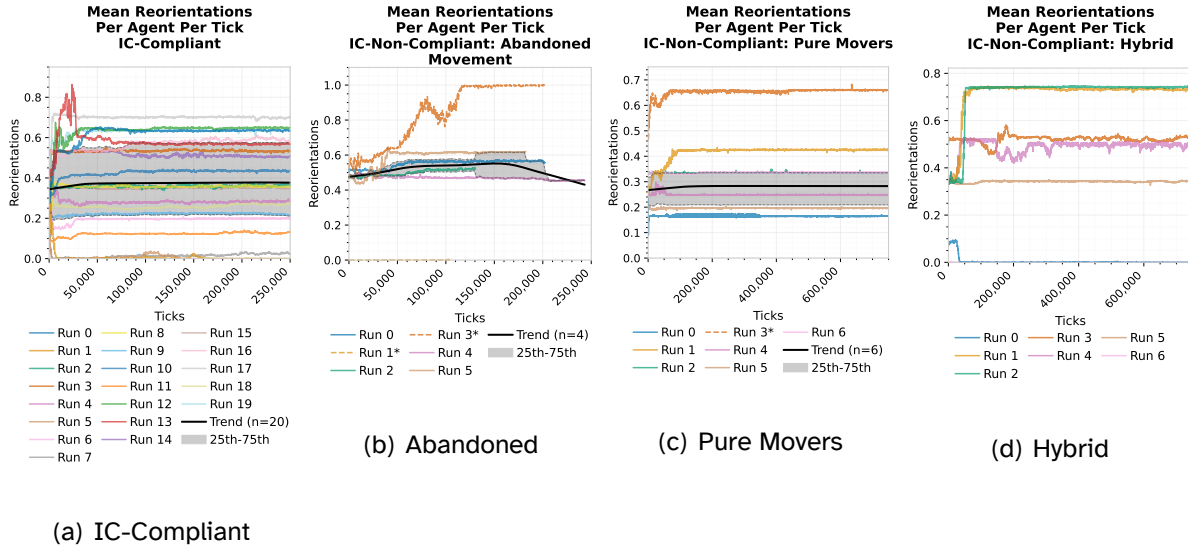


Figure 17: Average reorientations per agent (larger graphs in Appendix B)

729 As with the other metrics, all runs begin with a period of volatility in the reorientation
 730 rate, before plateauing at some relatively stable value. However, unlike all other metrics,
 731 there is no consistent trend between runs, even within their clusters. Agents settle on
 732 reorientation rates across the entire range. This is interesting because Crawlers, Sweepers,
 733 and Switchers were observed to emerge consistently across many runs, despite drastic
 734 differences in reorientation rate. By corollary agents in different runs are achieving the
 735 same population-level forms through different combinations of reorientations, replications,
 736 transfers, and (possibly) movement. This may explain the distinct evolutionary pathways
 737 (clusters) observed in IC-non-compliant runs, despite their initially similar appearance:
 738 some combinations are more easily mutated into pure replicate-and-transfer based
 739 strategies than others.

740 **11 Limitations**

741 Two key methodological constraints limit the generalisability of our findings:

- 742 • Mutation and crossover rates are tied to replication and mass transfer actions,
743 respectively. This coupling significantly reduces evolutionary pressure on pure
744 Mover populations, which don't need to replicate as often, whilst Hybrid strategies
745 experience intermediate pressure. This may have contributed to their plateauing at
746 lower neural complexity.
- 747 • The environment is small, homogeneous, and was constrained in its design in that it
748 had to be readily solvable by randomised initial agents in both variants. As such, it
749 provides little challenge to Switchers, and seemingly no opportunities to diversify or
750 improve the search strategy further.

751 **12 Conclusion**

752 Our experimental results provide strong support for the Interdependence Condition (IC)
753 as a framework for scaffolding the evolution of population-level complexity in artificial
754 life systems. The reliable emergence of superagency in the IC-compliant Myxomatrix,
755 characterised by the progression from Blobs to Crawlers to Sweepers and ultimately
756 to Switchers, demonstrates that enforced agent interdependence through emergent
757 dynamics can successfully guide evolutionary processes toward increasingly sophisticated
758 collective behaviours and ultimately superagency.

759 The Switcher pattern represents a particularly compelling example of evolved complexity,
760 exhibiting both novel collective capabilities and altruistic inter-lineage relationships.
761 These agents developed the ability to dynamically adjust their search patterns based on
762 resource distribution—a perception-decision-action loop that exists only at the population
763 level—while also displaying evolutionarily novel forms of altruism through mass transfer
764 between lineages. This achievement of non-trivial population-level complexity emerged
765 despite the potential genetic costs associated with inter-lineage mass transfer, suggesting
766 that the survival advantages of collective behaviour outweighed the risks to genetic

767 integrity.

768 Conversely, our analysis of the IC-non-compliant variant revealed that when agents
769 can develop independent survival strategies, they tend to settle into evolutionarily
770 stable states characterised by individualistic behaviours and significantly lower network
771 complexity. Even in cases where hybrid strategies emerged, combining movement with
772 replication and transfer, these populations consistently failed to develop superagency. The
773 tendency for mutations promoting formation-based strategies to be subverted back toward
774 individualistic behaviours, and for hybrid agents such as diffuse sweepers to maintain 1-cell
775 gaps and thereby prevent superagency, strongly support our hypothesis.

776 These findings suggest that the absence of complex population-level dynamics in previous
777 artificial life systems may be partially attributed to their initialisation with independently
778 viable agents. When individuals can survive and reproduce without relying on
779 population-level emergent properties, they appear to actively resist evolutionary pathways
780 that could lead to sophisticated collective behaviours, even when such behaviours
781 are mechanically possible, accessible through minor mutation, and competitively
782 advantageous once established.

783 The success of the IC in scaffolding the evolution of complexity offers useful insights
784 for designing future artificial life systems. By preventing agents from developing purely
785 individualistic strategies, the IC maintains population-level emergent properties that
786 seem to promote the evolution of collective behaviours. However, our relatively simple
787 environment suggests that more varied and challenging conditions might be needed to
788 drive the evolution of strategies more complex than the Switcher pattern. These results
789 help us understand how collective behaviours can emerge through evolution and provide
790 a practical approach for creating artificial life systems that more consistently develop
791 sophisticated population-level dynamics.

792 **13 Future Work**

793 Our findings suggest several promising directions for future research that could both
794 validate and expand upon the IC's role in scaffolding population-level complexity.

795 **13.1 Heterogeneous Environments**

796 We suppose that further superagent evolution is mechanically possible in the Myxomatrix,
797 but that the uniform and plentiful environment used in the tests in this work does
798 not provide adequate selection pressures to encourage it. Future work should explore
799 harsher environments, such as heterogenous ones with nurturing and harsh regions, or by
800 transferring agents into harsher environments once they plateau within a more nurturing
801 one. The nurturing regions would maintain current mechanics where Switchers reliably
802 evolve, while harsh regions would contain few, high-yield plants with long regrowth periods.

803 **13.2 Individual-Level Analysis**

804 This work has focused on population-level complexity, but individual-level complexity and
805 activity statistics should still be analysed in the Myxomatrix. Such analysis would help
806 quantify the relationship between individual and population-level complexity.

807 **13.3 Further Validating the IC**

808 The Myxomatrix provides a single test case for the IC; implemented through constraints
809 on agent mechanics. As ALife worlds are complex and complexifying systems, setting
810 up any IC experiment will potentially introduce confounding factors. As such, future
811 research should examine the IC's effects across fundamentally different implementation
812 approaches. One approach would be to implement the IC through environment design
813 rather than mechanical constraints, with one environment where cooperation is essential,

814 and another where it is merely beneficial. This would help distinguish the IC's general
815 principles from implementation-specific effects, and potentially suggest refinements for
816 the IC.

817 **14 Potentialities**

818 **14.1 Mutualistic Evolution of Individual and Population-Level 819 Complexity**

820 An important avenue for future work lies in investigating whether sophisticated
821 individual-level capabilities can coevolve with population-level complexity in IC-compliant
822 systems. This would require designing environments that both enforce the IC and provide
823 opportunities for extensive and varied individual agency, potentially revealing synergies
824 between individual and collective complexity evolution.

825 **14.2 Applications in Distributed Systems Engineering**

826 The Myxomatrix demonstrates the evolution of simple individual behaviours giving rise
827 to complex collective outcomes. Future research should explore whether IC-compliant
828 artificial life worlds may be designed to evolve practically useful collective behaviours,
829 such as rule-sets for agents in multi-agent distributed computational systems. The
830 T2Tile project (Ackley, 2021) for instance, which aims to produce an indefinitely scalable
831 multi-agent-based computational stack, employs a grid-based system similar to the
832 Myxomatrix.

833 **References**

- 834 Ackley, D. H. (2021). T2 tile project: A distributed computing platform using physical tiles
835 with robust-first architecture [Accessed July 1, 2025]. <https://t2tile.org/>
- 836 Bedau, M. A., McCaskill, J. S., Packard, N. H., Rasmussen, S., Adami, C., Green, D. G., Ikegami,
837 T., Kaneko, K., & Ray, T. S. (2000). Open problems in artificial life. *Artificial Life*, 6(4),
838 363–376. <https://doi.org/10.1162/106454600300103683>
- 839 Blokhuis, A., Lacoste, D., & Nghe, P. (2020). Universal motifs and the diversity of
840 autocatalytic systems. *Proceedings of the National Academy of Sciences*, 117(41),
841 25230–25236.
- 842 Boisseau, R. P., Vogel, D., & Dussutour, A. (2016). Habituation in non-neural organisms:
843 Evidence from slime moulds. *Proceedings of the Royal Society B: Biological
844 Sciences*, 283(1829), 20160446. <https://doi.org/10.1098/rspb.2016.0446>
- 845 Bonabeau, E., Dorigo, M., & Theraulaz, G. (1999). *Swarm intelligence: From natural to
846 artificial systems*. Oxford University Press.
- 847 Boussard, A., Fessel, A., Oettmeier, C., Briard, L., Döbereiner, H.-G., & Dussutour, A.
848 (2021). Adaptive behaviour and learning in slime moulds: The role of oscillations.
849 *Philosophical Transactions of the Royal Society B*, 376(1820), 20190757. <https://doi.org/10.1098/rstb.2019.0757>
- 850 Brockman, G., Cheung, V., Pettersson, L., Schneider, J., Schulman, J., Tang, J., & Zaremba, W.
851 (2016). OpenAI Gym. *arXiv preprint arXiv:1606.01540*.
- 852 Caussan, L. (2020). The bibites [Accessed: 5 April 2024]. <https://thebibites.itch.io/the-bibites>
- 853 Channon, A. (2001). Passing the ALife test: Activity statistics classify evolution in Geb
854 as unbounded. *Advances in Artificial Life: 6th European Conference, ECAL 2001*,
855 417–426.
- 856 Channon, A. (2019). Maximum individual complexity is indefinitely scalable in Geb. *Artificial
857 Life*, 25(2), 134–144.

- 860 Darwin, C. (1859). *On the origin of species by means of natural selection, or the*
861 *preservation of favoured races in the struggle for life*. John Murray.
- 862 Detrain, C., & Deneubourg, J.-L. (2006). Self-organized structures in a superorganism: Do
863 ants “behave” like molecules? *Physics of Life Reviews*, 3(3), 162–187. <https://doi.org/10.1016/j.plrev.2006.07.001>
- 864 Eigen, M., & Schuster, P. (1979). The hypercycle: A principle of natural self-organization.
865 *Naturwissenschaften*, 66, 58–77.
- 866 Ewert, W., Dembski, W. A., & Marks II, R. J. (2013). Tierra: The character of adaptation. In
867 *Biological information: New perspectives* (pp. 105–138).
- 868 Fernández, N., Maldonado, C., & Gershenson, C. (2014). Information measures of
869 complexity, emergence, self-organization, homeostasis, and autopoiesis. In *Guided*
870 *self-organization: Inception* (pp. 19–51). Springer Berlin Heidelberg.
- 871 Gardner, A., & Grafen, A. (2009). Capturing the superorganism: A formal theory of group
872 adaptation. *Journal of Evolutionary Biology*, 22(4), 659–671. <https://doi.org/10.1111/j.1420-9101.2008.01681.x>
- 873 Goldberg, D. E. (1989). *Genetic algorithms in search, optimization and machine learning*.
874 Addison-Wesley.
- 875 Hamilton, W. D. (1971). Geometry for the selfish herd. *Journal of Theoretical Biology*, 31(2),
876 295–311.
- 877 Hordijk, W. (2013). Autocatalytic sets: From the origin of life to the economy. *BioScience*,
878 63(11), 877–881.
- 879 Huxley, J. (1942). *Evolution: The modern synthesis*. Allen & Unwin.
- 880 Jain, S., & Krishna, S. (1998). Autocatalytic sets and the growth of complexity in an
881 evolutionary model. *Physical Review Letters*, 81(25), 5684.
- 882 Lopez-Ruiz, R., Mancini, H. L., & Calbet, X. (1995). A statistical measure of complexity.
883 *Physics Letters A*, 209(5-6), 321–326.
- 884 Lush, J. L. (1943). *Animal breeding plans* (2nd ed.). Iowa State College Press.

- 887 Maass, W. (1997). Networks of spiking neurons: The third generation of neural network
888 models. *Neural Networks*, 10(9), 1659–1671.
- 889 Markovitch, O., & Lancet, D. (2012). Excess mutual catalysis is required for effective
890 evolvability. *Artificial Life*, 18(3), 243–266.
- 891 Mitchell, M. (1998). *An introduction to genetic algorithms*. MIT Press.
- 892 Ofria, C., & Wilke, C. O. (2004). Avida: A software platform for research in computational
893 evolutionary biology. *Artificial Life*, 10(2), 191–229.
- 894 Packard, N., Bedau, M. A., Channon, A., Ikegami, T., Rasmussen, S., Stanley, K. O., &
895 Taylor, T. (2019). An overview of open-ended evolution: Editorial introduction to the
896 open-ended evolution ii special issue. *Artificial Life*, 25(2), 93–103.
- 897 Peng, Z., Linderoth, J., & Baum, D. A. (2022). The hierarchical organization of autocatalytic
898 reaction networks and its relevance to the origin of life. *PLoS Computational Biology*,
899 18(9), e1010498.
- 900 Plasson, R., Brandenburg, A., Jullien, L., & Bersini, H. (2011). Autocatalysis: At the root of
901 self-replication. *Artificial Life*, 17(3), 219–236.
- 902 Ray, T. S. (1991). An approach to the synthesis of life. *Artificial Life II*, 11, 371–408.
- 903 Reid, C. R., Sumpter, D. J. T., & Beekman, M. (2011). Optimisation in a natural system:
904 Argentine ants solve the Towers of Hanoi. *Journal of Experimental Biology*, 214(1),
905 50–58. <https://doi.org/10.1242/jeb.048173>
- 906 Rose, M. R., & Oakley, T. H. (2007). The new biology: Beyond the modern synthesis. *Biology
907 Direct*, 2, 1–17. <https://doi.org/10.1186/1745-6150-2-30>
- 908 Shannon, C. E. (1948). A mathematical theory of communication. *The Bell System Technical
909 Journal*, 27(3), 379–423.
- 910 Song, S., Miller, K. D., & Abbott, L. F. (2000). Competitive Hebbian learning through
911 spike-timing-dependent synaptic plasticity. *Nature Neuroscience*, 3(9), 919–926.
912 <https://doi.org/10.1038/78829>

- 913 Soros, L. B., & Stanley, K. O. (2014). Identifying necessary conditions for open-ended
914 evolution through the artificial life world of chromaria. *Artificial Life Conference*
915 *Proceedings 14*, 793–800.
- 916 Stanley, K. O., & Miikkulainen, R. (2002). Evolving neural networks through augmenting
917 topologies. *Evolutionary Computation*, 10(2), 99–127.
- 918 Szathmáry, E., & Smith, J. M. (1997). From replicators to reproducers: The first major
919 transitions leading to life. *Journal of Theoretical Biology*, 187(4), 555–571.
- 920 Taylor, T., Bedau, M., Channon, A., Ackley, D., Banzhaf, W., Beslon, G., Dolson, E., Froese,
921 T., Hickinbotham, S., Ikegami, T., et al. (2016). Open-ended evolution: Perspectives
922 from the OEE workshop in York. *Artificial Life*, 22(3), 408–423. https://doi.org/10.1162/ARTL_a_00210
- 923 Wallace, A. R. (1858). On the tendency of varieties to depart indefinitely from the original
924 type. *Journal of the Proceedings of the Linnean Society of London. Zoology*, 3(9),
925 53–62. <https://doi.org/10.1111/j.1096-3642.1858.tb02500.x>
- 926 West, S. A., Griffin, A. S., & Gardner, A. (2007). Evolutionary explanations for cooperation.
927 *Current Biology*, 17(16), R661–R672.
- 928 Yaeger, L. (1994). Computational genetics, physiology, metabolism, neural systems,
929 learning, vision, and behavior or PolyWorld: Life in a new context. *Artificial Life III*,
930 263–298.
- 931

932 **A Indefinite NeuroEvolution of Augmenting** 933 **Spike-Timing-Dependent Plastic Topologies** 934 **(INEASTDPT)**

935 Previous artificial life worlds have employed various genetic representations, ranging
936 from programs with mutable instructions (Tierra, Avida, Evita) to genetically encoded

937 neural networks. Recent works, such as Chromaria, have predominantly used NEAT and
938 its variants to encode neural networks that each control and influence the attributes
939 of an agent within some simulated environment. NEAT encodes conventional artificial
940 neural networks (multilayer perceptrons, ANNs), facilitating mutation, crossover between
941 parent representations, and quantification of genetic disparity between representations.
942 However, concerning artificial life worlds, the NEAT approach has two significant
943 limitations:

- 944 • It relies on a global innovation counter, which impedes parallelism due to race
945 conditions and limits maximum runtime as unique innovation numbers will eventually
946 be exhausted.
- 947 • ANNs are less suited to event-driven cognition within (approximately) spatially and
948 temporally continuous environments than spiking neural networks (SNNs), which
949 better approximate biological neural networks (Maass, 1997). Some SNN models,
950 such as Spike Timing Dependent Plasticity (STDP) (Song et al., 2000), facilitate
951 biologically realistic Hebbian weight updates based on synaptic activity.

952 We present Indefinite NeuroEvolution of Augmenting Spike Timing Dependent Plastic
953 Topologies (INEASTDPT), a NEAT variant designed for open-ended evolution in
954 event-driven environments. This model eliminates the global innovation number and
955 represents STDP networks with mutable Hebbian learning parameters. INEASTDPT
956 was validated using a conventional genetic algorithm approach to the classic CartPole
957 benchmarking environment from OpenAI Gymnasium (Brockman et al., 2016) before its
958 application in this work.

959 **A.1 Representation**

960 INEASTDPT maintains two lists per representation:

- 961 • **Neural:** Holds integrate-and-fire neurons; initially contains only input and output

962 nodes.

963 • **Synaptic:** Holds plastic synapses; initially empty.

964 Each neuron is associated with some number of input and output synapses from the
965 synaptic list.

966 Each synapse is associated with one pre- and one post-synaptic neuron from the neural
967 list; they are unidirectional.

968 A neuron associates with each of its input synapses as a post-synaptic neuron, and each
969 of its output synapses as a pre-synaptic neuron.

970 Elements in each list are associated with elements in the other list based on their positions
971 within their respective list. Both lists may include null elements as placeholders for deleted
972 neurons or synapses, as illustrated in Tables 2 and 3. These null elements maintain
973 positional integrity when elements are removed by mutation.

974 Synapses associated with null neural position(s) are redundant and are ignored when
975 building a network from the representation, while nodes associated with null synaptic
976 position(s) have no effect.

Network Diagram

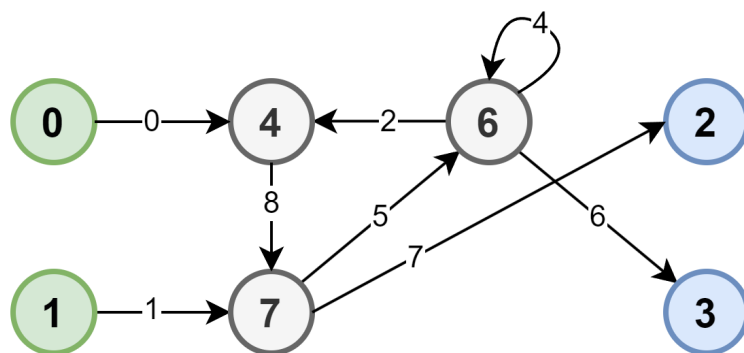


Figure 18: A diagram of an INEASTDPT neural network, showing the positions of each neuron and synapse in the neural and synaptic lists, respectively (see Tables 2 and 3, respectively).

Neurons

Position	0	1	2	3	4	5	6	7
Type	I	I	O	O	H	N	H	H
Inputs	-	-	7	6	0	-	4,5	1
Outputs	0	1	-	-	8	-	2,4,6	5,7

Table 2: The neural list for the INEASTDPT network depicted in Figure 18, showing each neuron's position, type (see Table 4 for legend), and its associated input and output positions in the synaptic list (see Table 3).

Synapses

Position	0	1	2	3	4	5	6	7	8
Type	S	S	S	N	S	S	S	S	S
Pre	0	1	6	-	6	7	6	7	4
Post	4	7	4	-	6	6	3	2	7

Table 3: The synaptic list for the INEASTDPT network depicted in Figure 18, showing each synapse's position, type (see Table 4 for legend), and its associated pre- and post-synaptic positions in the neural list (see Table 2).

Legend

Type	Description
I	Input Neuron
O	Output Neuron
H	Hidden Neuron
S	Synapse
N	Null Element

Table 4: Legend for element types in the neural and synaptic lists.

977 **A.2 Mutation Operations**

978 The following mutation operations are implemented:

- 979 • Randomising or nudging synapse parameters: weight, pre-, and post-synaptic
980 learning rates.
- 981 • Randomising or nudging neuron biases.
- 982 • Creating new hidden neurons and synapses, in their respective lists.
- 983 • Deleting hidden neurons and synapses.
- 984 • Duplicating hidden neurons and their synapses.

985 If an element is deleted by mutation it is replaced with a null element. After a deletion,
986 any null elements at the end of the list are removed.

987 When a new element is created by mutation it replaces the first null element, or if no
988 positions hold a null element then the list is extended.

989 **A.3 Crossover Operations**

990 Crossover operations exchange information between corresponding positions in the
991 neural/synaptic lists of two parent representations.

- 992 • **Attribute Crossover:** Applied to the neural and synaptic lists independently. Swaps
993 the biases of a pair of nodes, or the weight, pre-, and post-synaptic learning rates of
994 a pair of connections.
- 995 • **Topology Crossover:** Applied to the neural list. Swaps nodes at a given position,
996 including null nodes, and exchanges all of the synapses associated with those nodes.
997 If the position of an associated synapse is in use in the representation into which it is
998 transferred (i.e. that position contains a connection associated with a node not being
999 crossed), then it is placed in the first available position, and the node's association

1000 is reconfigured accordingly. This method allows functional network topology to be
1001 crossed.

1002 **A.4 Crossover Application Methods**

1003 Both attribute and topology crossover can be applied between two parent representations,
1004 to produce two offspring representations, in the following ways:

- 1005 • **Uniform:** Applies crossover at each position with a given probability
- 1006 • **N-Point:** Segments the parent lists at N random positions and applies crossover at
1007 every position in every other segment.
- 1008 • **N-Random:** Applies crossover at N randomly selected positions.

1009 **A.5 Genetic Comparison**

1010 The INEASTDPT model represents controller networks as two lists: one for nodes and one
1011 for connections. The genetic similarity between two network representations is calculated
1012 based on the number of disjointed elements and parameter disparities between matching
1013 elements.

1014 Two neurons are considered matching if they are each associated with the same input and
1015 output synaptic positions. Similarly, two synapses match if they connect the same pre- and
1016 post-synaptic neural positions within their respective lists. Otherwise, they are disjointed.

1017 Corresponding null positions are ignored, while an element in one list corresponding to a
1018 null or non-existent position in the other is considered disjoint.

1019 The genetic disparity Δ between two networks A and B is calculated as follows:

1020 D_n and D_s denote the proportion of neurons and synapses, respectively, that are disjointed

1021 between networks A and B :

$$D_n = \frac{|D_n|}{|D_n| + |M_n|}, \quad D_s = \frac{|D_s|}{|D_s| + |M_s|} \quad (1)$$

1022 where:

1023 • D_n and D_s are the sets of disjointed neurons and synapses, respectively.

1024 • M_n and M_s are the sets of matching neurons and synapses, respectively.

1025 δ_b denotes the disparity between the biases of matching neurons, normalised over the total

1026 number of matching and disjointed neurons:

$$\delta_b = \frac{\sum_{i \in M_n} |b_{A,i} - b_{B,i}|}{|D_n| + |M_n|} \quad (2)$$

1027 where $b_{A,i}, b_{B,i}$ are the biases of matching neuron i in networks A and B , respectively.

1028 δ_w , δ_{pre} , and δ_{post} denote the disparities between the weights, presynaptic learning rates,

1029 and postsynaptic learning rates of matching synapses, respectively, normalised over the

1030 total number of matching and disjointed synapses:

$$\delta_w = \frac{\sum_{i \in M_s} |w_{A,i} - w_{B,i}|}{|D_s| + |M_s|} \quad (3)$$

1031

$$\delta_{pre} = \frac{\sum_{i \in M_s} |r_{pre,A,i} - r_{pre,B,i}|}{|D_s| + |M_s|}, \quad \delta_{post} = \frac{\sum_{i \in M_s} |r_{post,A,i} - r_{post,B,i}|}{|D_s| + |M_s|} \quad (4)$$

1032 where:

1033 • $w_{A,i}, w_{B,i}$ are the weights of matching synapse i in networks A and B , respectively.

1034 • $r_{pre,A,i}, r_{pre,B,i}$ are the presynaptic learning rates of matching synapse i in networks
1035 A and B , respectively.

1036 • $r_{post,A,i}, r_{post,B,i}$ are the postsynaptic learning rates of matching synapse i in networks

1037 A and B , respectively.

1038 Finally, we calculate the overall genetic disparity $\Delta(A, B)$ between networks A and B :

$$\Delta_n(A, B) = \frac{c_n D_n + c_b \delta_b}{2} \quad (5)$$

1039 $\Delta_s(A, B) = \frac{c_s D_s + c_w \delta_w + c_{pre} \delta_{pre} + c_{post} \delta_{post}}{4} \quad (6)$

1040 $\Delta(A, B) = \frac{\Delta_s(A, B) + \Delta_n(A, B)}{2} \quad (7)$

1041 where:

- 1042 • $\Delta_n(A, B)$ is the neuron-level disparity
- 1043 • $\Delta_s(A, B)$ is the synapse-level disparity
- 1044 • c_n is the coefficient weighting disjointed neurons
- 1045 • c_b is the coefficient weighting matching neuron bias disparity
- 1046 • c_s is the coefficient weighting disjointed synapses
- 1047 • c_w is the coefficient weighting matching synapse weight disparity
- 1048 • c_{pre} is the coefficient weighting matching synapse presynaptic learning rate disparity
- 1049 • c_{post} is the coefficient weighting matching synapse postsynaptic learning rate disparity

1051 Two networks are considered compatible if $\Delta(A, B)$ does not exceed a given threshold θ :

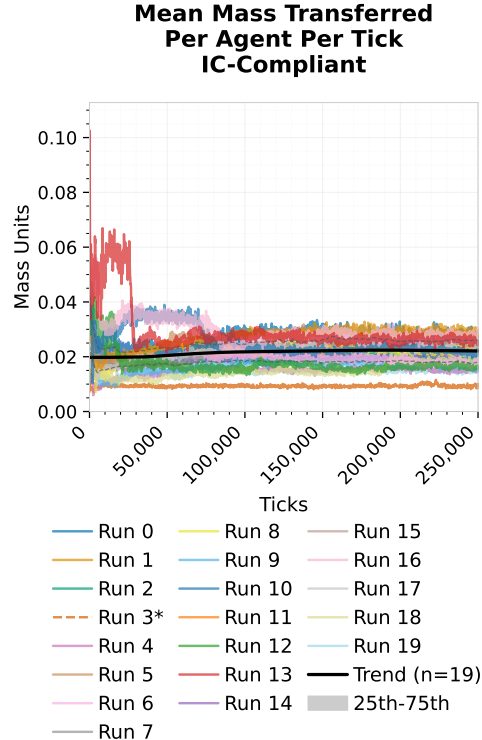
$$\text{Compatible}(A, B) = \begin{cases} \text{True}, & \text{if } \Delta(A, B) \leq \theta \\ \text{False}, & \text{otherwise} \end{cases} \quad (8)$$

1052 This representation allows for flexible evolution of network STDP topologies while

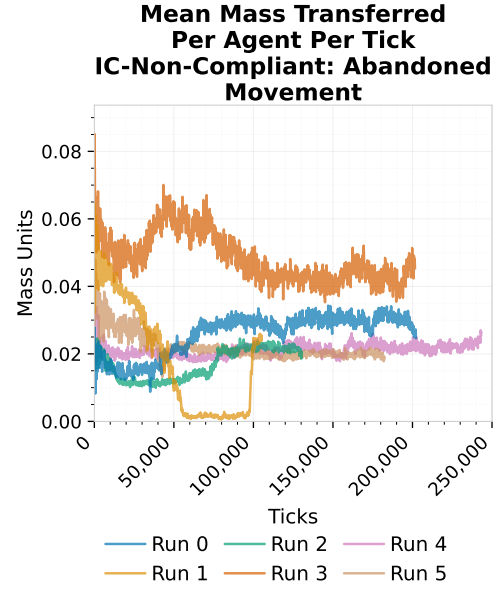
¹⁰⁵³ maintaining a measure of genetic similarity for speciation.

1054 **B Enlarged Figures**

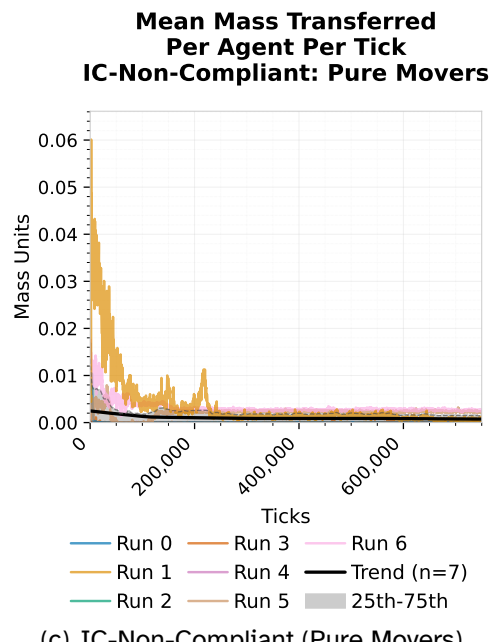
1055 **B.1 Mass Transfer Analysis**



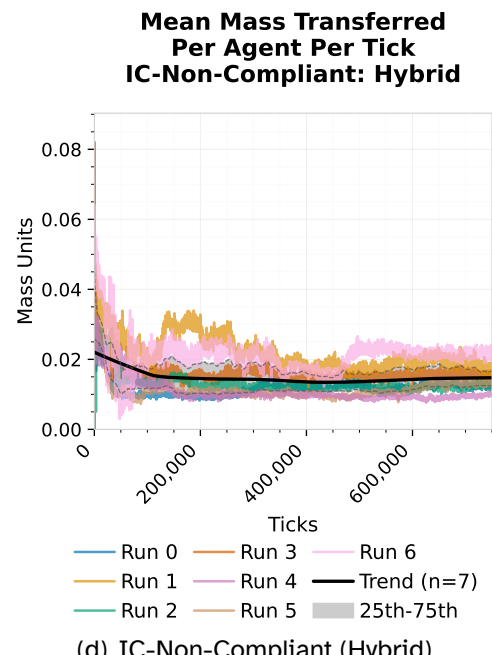
(a) IC-Compliant (Combined)



(b) IC-Non-Compliant (Abandoned)



(c) IC-Non-Compliant (Pure Movers)



(d) IC-Non-Compliant (Hybrid)

Figure 19: Average mass transferred per agent across all simulation variants (detailed view)

B.2 Replication Analysis

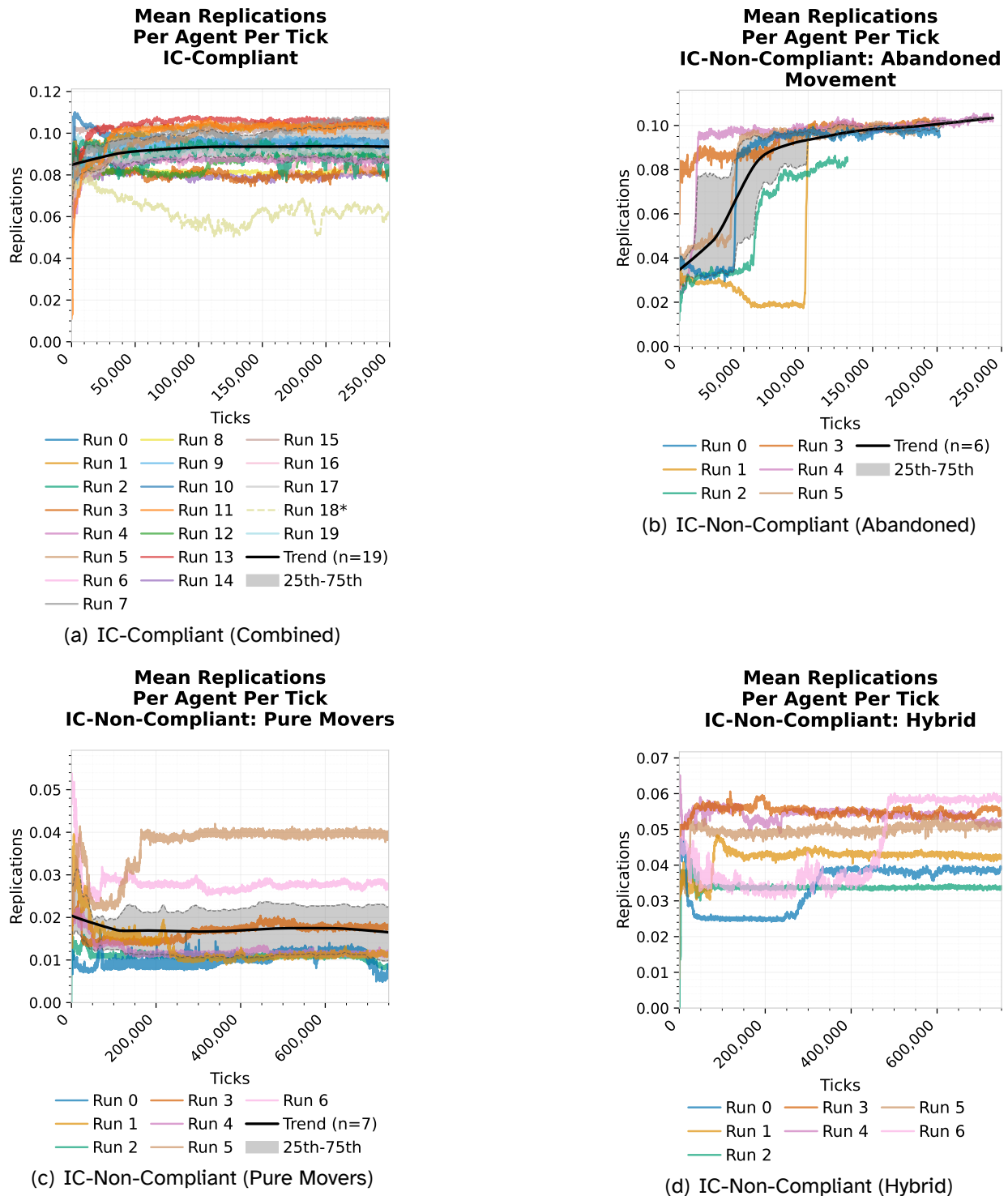


Figure 20: Average replications per agent across all simulation variants (detailed view)

B.3 Movement Analysis

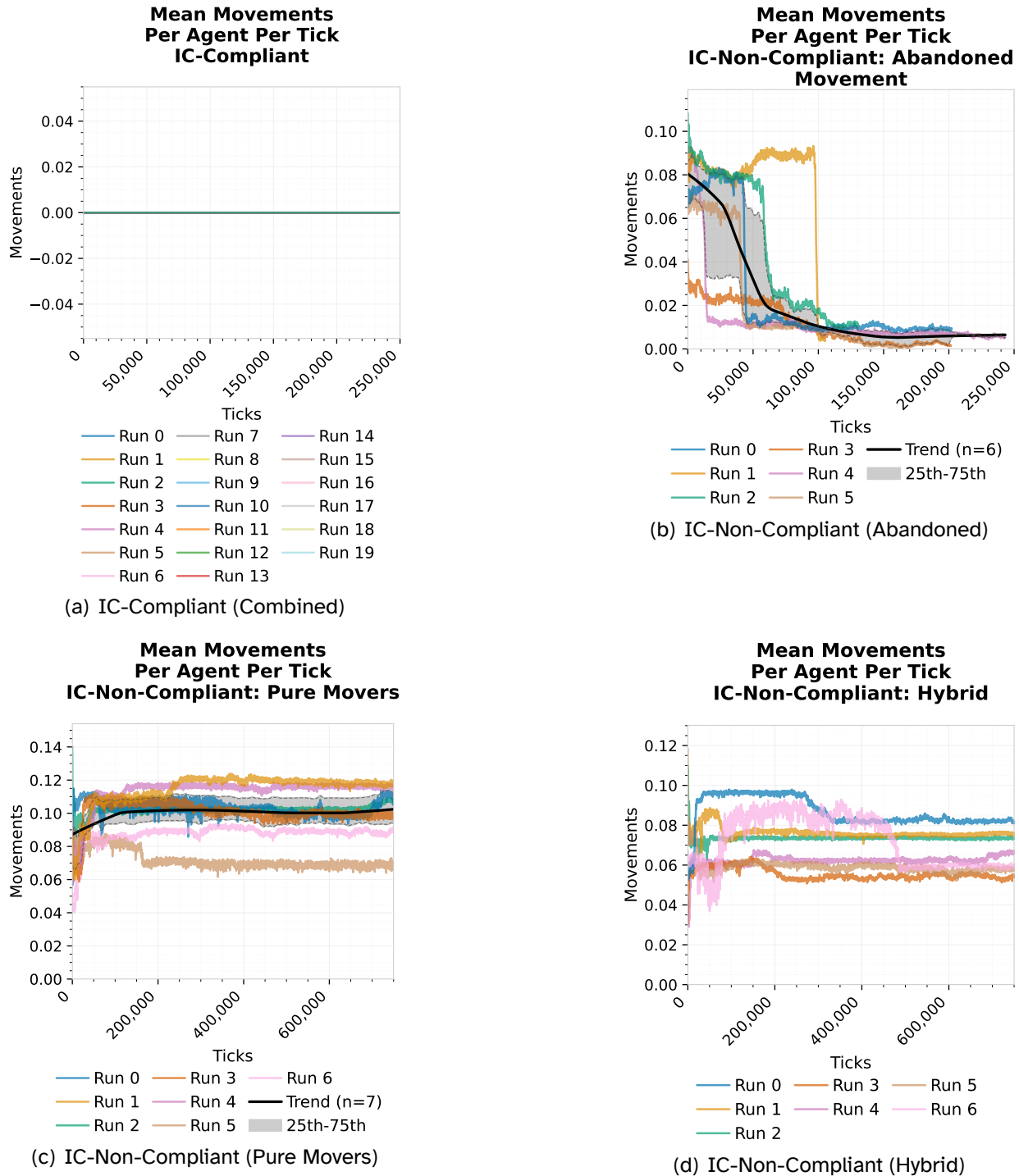


Figure 21: Average movements per agent across all simulation variants (detailed view)

B.4 Population Size Analysis

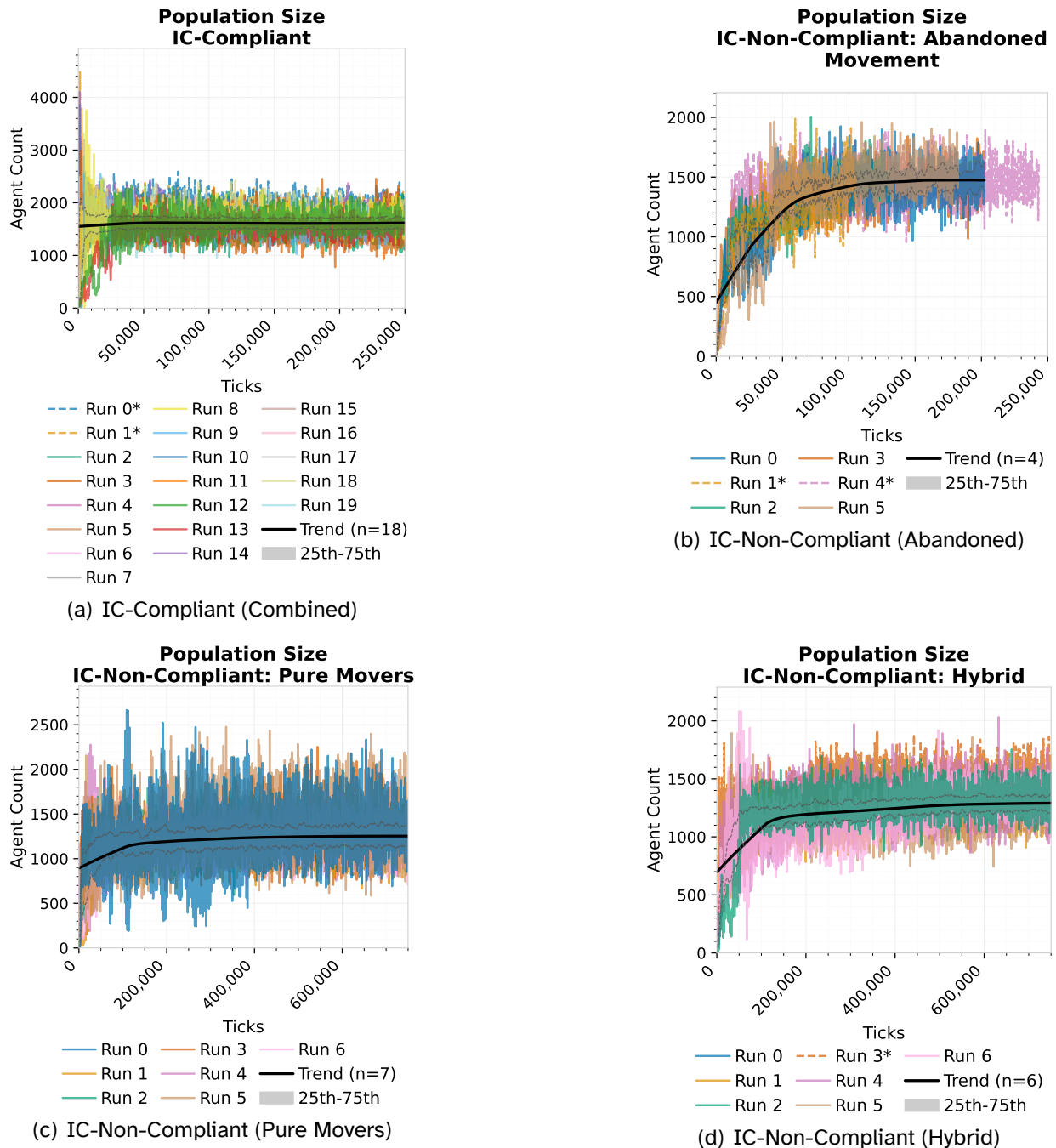
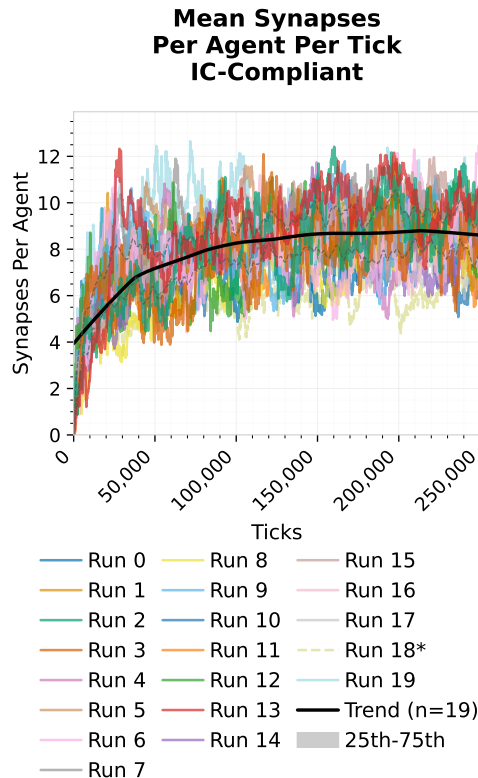


Figure 22: Population size over time across all simulation variants (detailed view)

B.5 Synapses Analysis



(a) IC-Compliant (Combined)

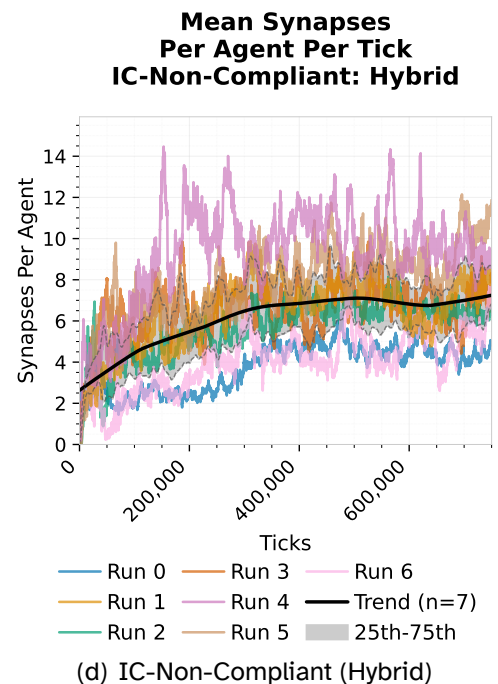
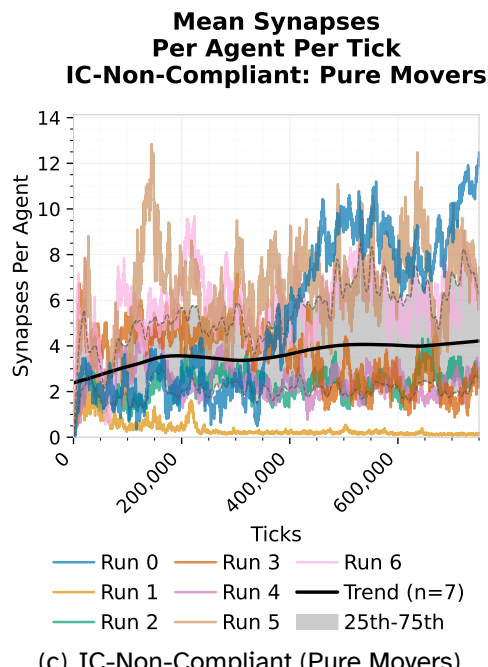
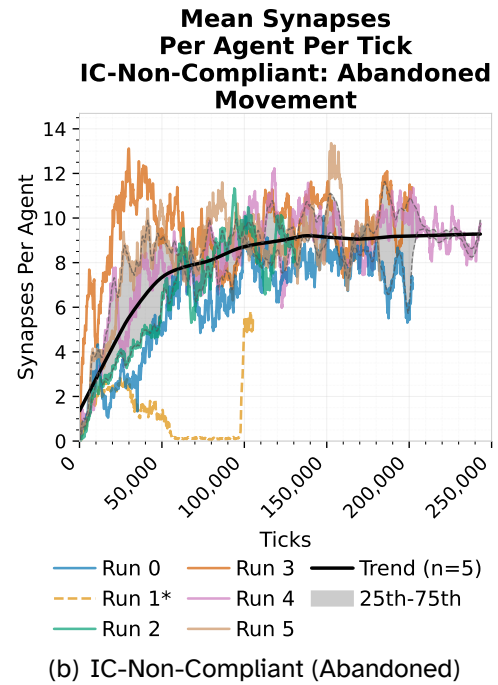
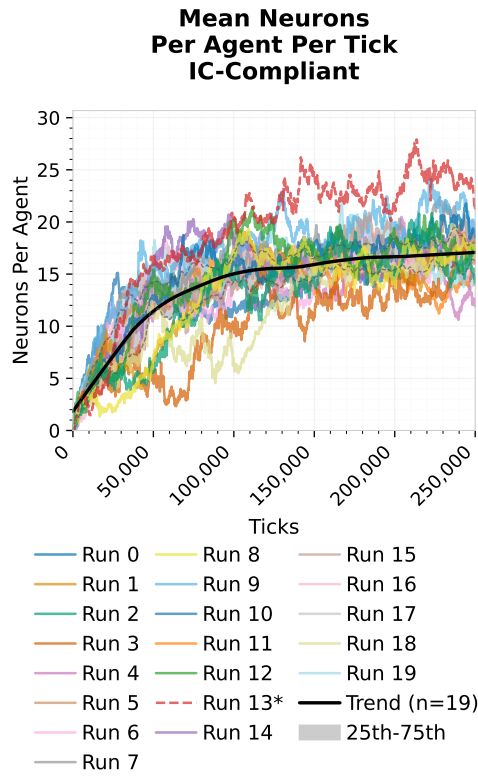


Figure 23: Average number of synapses per agent across all simulation variants (detailed view)

B.6 Hidden Neurons Analysis



(a) IC-Compliant (Combined)

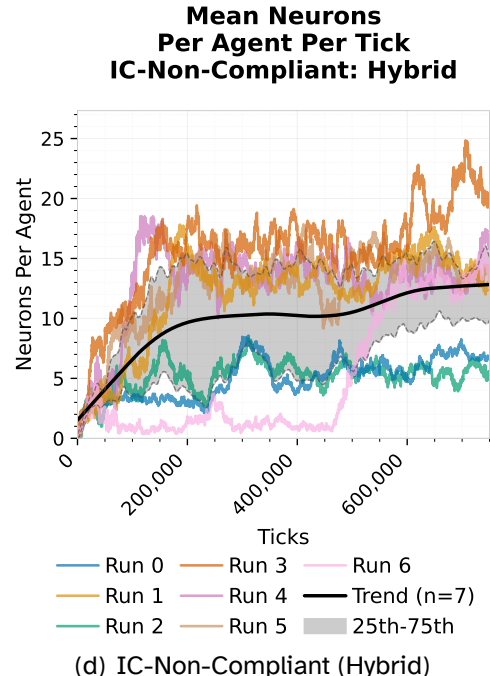
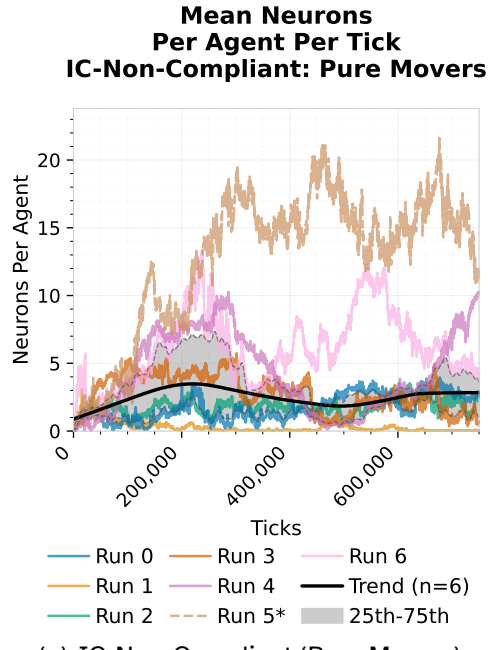
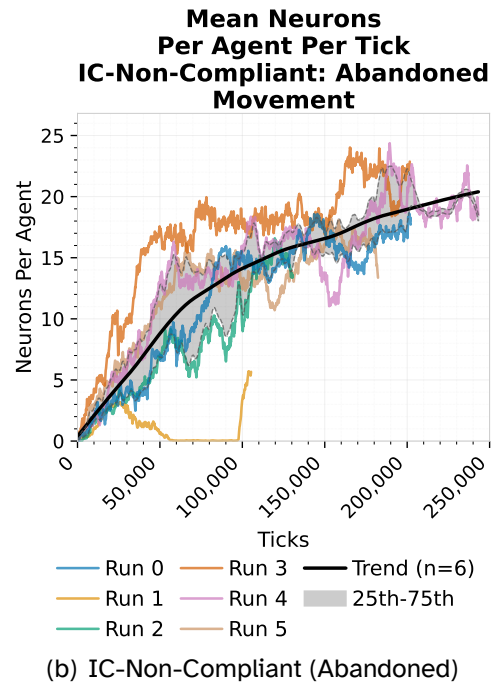


Figure 24: Average number of neurons per agent across all simulation variants (detailed view)

B.7 Communication Analysis

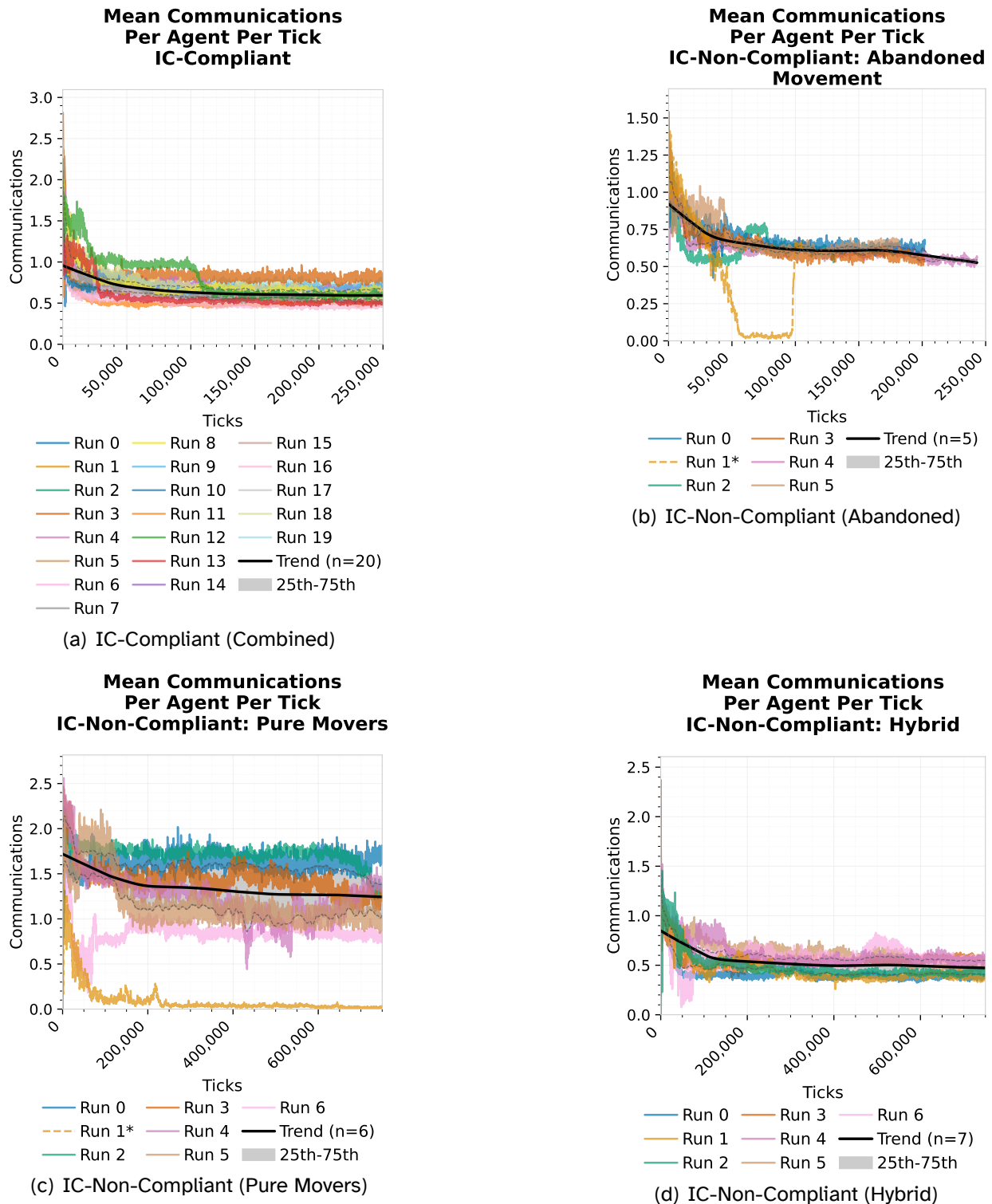
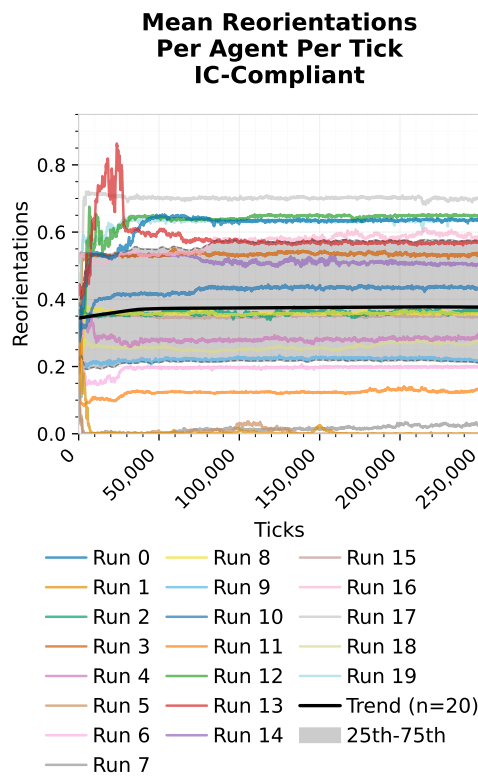
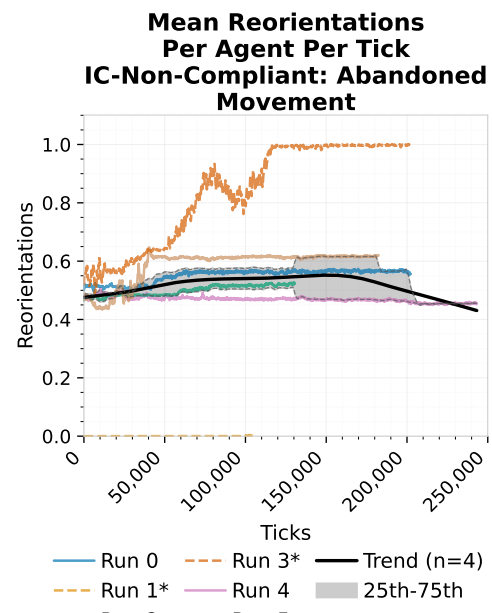


Figure 25: Average communications per agent across all simulation variants (detailed view)

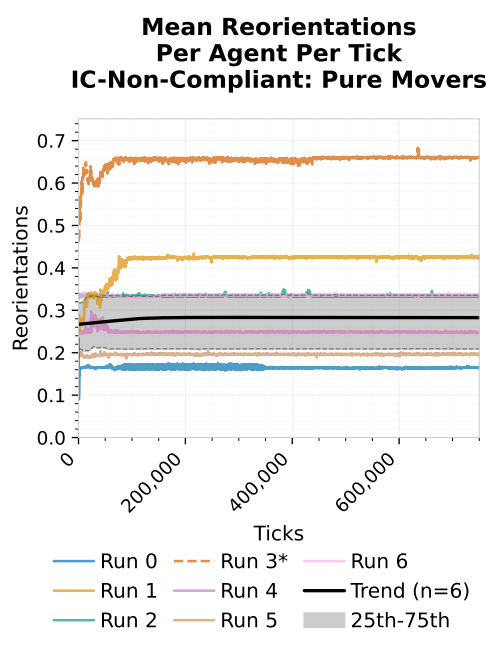
B.8 Reorientation Analysis



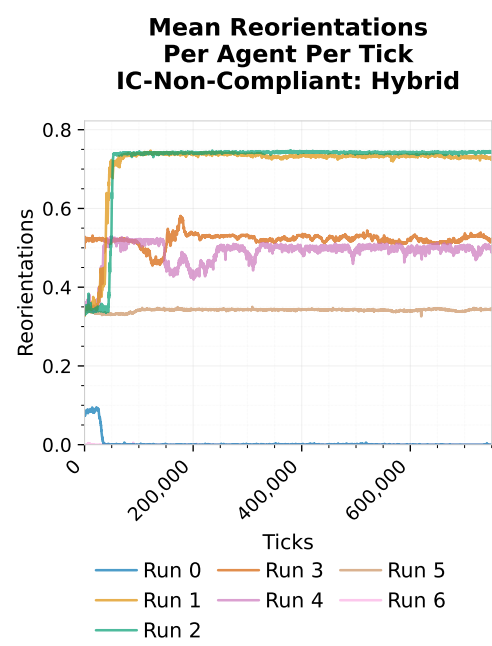
(a) IC-Compliant (Combined)



(b) IC-Non-Compliant (Abandoned)



(c) IC-Non-Compliant (Pure Movers)



(d) IC-Non-Compliant (Hybrid)

Figure 26: Average reorientations per agent across all simulation variants (detailed view)